

**Lidar turbulence
measurements
review**

A. Sathe and J. Mann

This discussion paper is/has been under review for the journal Atmospheric Measurement Techniques (AMT). Please refer to the corresponding final paper in AMT if available.

A review of turbulence measurements using ground-based wind lidars

A. Sathe and J. Mann

DTU Wind Energy, Risø campus, Roskilde, Denmark

Received: 29 May 2013 – Accepted: 9 July 2013 – Published: 26 July 2013

Correspondence to: A. Sathe (amsat@dtu.dk)

Published by Copernicus Publications on behalf of the European Geosciences Union.

Title Page

Abstract

Introduction

Conclusions

References

Tables

Figures

⏪

⏩

◀

▶

Back

Close

Full Screen / Esc

Printer-friendly Version

Interactive Discussion



Abstract

A review of turbulence measurements using ground-based wind lidars is carried out. Works performed in the last 30 yr, i.e. from 1972–2012 are analyzed. More than 80 % of the work has been carried out in the last 15 yr, i.e. from 1997–2012. New algorithms to process the raw lidar data were pioneered in the first 15 yr, i.e. from 1972–1997, where standard techniques could not be used to measure turbulence. Obtaining unfiltered turbulence statistics from the large probe volume of the lidars has been and still remains the most challenging aspect. Until now, most of the processing algorithms that have been developed have shown that by combining an isotropic turbulence model with raw lidar measurements, we can obtain unfiltered statistics. We believe that an anisotropic turbulence model will provide a more realistic measure of a turbulence statistic. Future development in algorithms will depend on whether the unfiltered statistics can be obtained without the aid of any turbulence model. With the tremendous growth of the wind energy sector, we expect that lidars will be used for turbulence measurements much more than ever before.

1 Introduction

This study is motivated by the recent growth in the use of wind lidars for wind energy purposes. Understanding and measuring atmospheric turbulence is vital to efficient harnessing of wind energy and to measuring the structural integrity of a wind turbine. Traditionally, meteorological mast (met-mast) anemometry has been used, where either cup or sonic anemometers are mounted on slender booms at one or several heights to measure turbulence over a certain period of time. For wind energy purposes, much interest is focused on the turbulence of the wind and temperature, although some interest is also given to other atmospheric variables such as pressure, humidity, density etc. In this article we focus our review only on the measurement of atmospheric turbulence of wind by ground-based wind lidars. To our knowledge there is no such dedicated review

AMTD

6, 6815–6871, 2013

Lidar turbulence measurements review

A. Sathe and J. Mann

Title Page

Abstract

Introduction

Conclusions

References

Tables

Figures

◀

▶

◀

▶

Back

Close

Full Screen / Esc

Printer-friendly Version

Interactive Discussion



article. Engelbart et al. (2007) provide an overall review of different remote sensing techniques for turbulence measurements including lidars, whereas Emeis et al. (2007) provide a review of the use of lidars for wind energy applications without focusing in particular on turbulence measurements.

5 Turbulence affects the wind turbines mainly in two ways, one is the fluctuations that are caused in the extracted wind power (Kaiser et al., 2007; Gottschall and Peinke, 2008), and second is the fluctuations in the loads on different components of a wind turbine (Sathe et al., 2012). These fluctuations result in inefficient harnessing of wind energy and have the potential to inflict fatigue damage. Wind turbines are generally designed for a period of twenty years (Burton et al., 2001; IEC, 2005a). The size of a wind turbine has grown significantly over the past few decades. The upper tip of a modern wind turbine blade can easily reach heights up to 200 m above the ground. Thus measuring and understanding the turbulent wind field at great heights is essential. It is very expensive to install and operate a met-mast at such great heights for a sustained period of time. Especially offshore, the costs increase significantly owing to the large foundation needed to support the met-mast. Moreover, a met-mast cannot be moved from one place to the other, thus limiting the range of studies. Measuring in the wake of a wind turbine (or multiple wakes) then becomes quite a challenge. Lidars have the potential to counter these disadvantages of the met-mast anemometry. Recently, lidars have been used extensively for wind energy purposes in the measurement of the mean wind speed and wind profiling (Smith et al., 2006; Kindler et al., 2007; Peña et al., 2009; Wagner et al., 2011). However, despite years of research all over the world (particularly for meteorological studies) they have not yet been accepted for turbulence measurements. Different reasons can be attributed to its lack of acceptance such as large measurement volumes leading to spatial averaging of turbulence along the line-of-sight of its measurement axis, cross-contamination by different components of the wind field, low sampling rates etc.

25 This article attempts to answer two research questions pertaining to measurement of atmospheric turbulence by ground-based wind lidars:

AMTD

6, 6815–6871, 2013

Lidar turbulence measurements review

A. Sathe and J. Mann

Title Page

Abstract

Introduction

Conclusions

References

Tables

Figures



Back

Close

Full Screen / Esc

Printer-friendly Version

Interactive Discussion



**Lidar turbulence
measurements
review**

A. Sathe and J. Mann

Title Page

Abstract

Introduction

Conclusions

References

Tables

Figures



Back

Close

Full Screen / Esc

Printer-friendly Version

Interactive Discussion



1. What is the state-of-the-art?

2. Are further improvements needed, either in lidar technology or data processing algorithms that can make turbulence measurements more reliable?

It is to be noted that the main focus is on the review of processing algorithms using the raw lidar data and different scanning configurations. Although it is known that different lidar parameters can also influence turbulence measurements (Frehlich, 1994; Banakh and Werner, 2005), no review is carried out with respect to the technology itself, but that to a certain extent can be found in Hardesty and Darby (2005).

In general for any variable (or a combination of different variables) turbulence is characterized in several ways, in the time domain as auto or cross correlation functions, turbulent kinetic energy dissipation rate, and structure functions, or in the Fourier space as one or multi-dimensional auto or cross spectrum. In the remaining article we will delve into these aspects in some detail. We believe that writing such a review article without including any mathematics will provide only a superficial explanation. Hence we have included some mathematics using a uniform set of notations, in order to provide a clear perspective of the past studies. To this extent, in Sect. 2 we define some mathematical preliminaries that characterize atmospheric turbulence. In Sect. 3 we provide some explanation of the standard scanning configurations that have been used in the past. Section 4 attempts to answer the first research question posed above. It is divided into two subsections, where at first we describe the pioneering works along with the corresponding mathematics, and then we classify the past studies based on the investigated turbulence parameters. Readers who are interested only in knowing the state-of-the-art without going into too much mathematical details can directly jump to Sect. 4.2. In Sect. 5, some perspectives are provided on the specific turbulence parameters that are useful for wind energy purposes. A summary is provided in Sect. 6, where we attempt to answer the second research question posed above.

2 Mathematical preliminaries

In this article we will often switch between the bold faced vector notation and the Einstein indicial notation. We define the wind field as $\mathbf{v} = (u, v, w)$, where we define the coordinate system to be right-handed such that u (longitudinal component) is in the x_1 direction, v (transversal component) is in the x_2 direction, and w is in the vertical x_3 direction (see Fig. 1). If we consider that the fluctuations of the wind field are homogeneous in space then the auto or cross covariance functions can be defined only in terms of the separation distance as,

$$R_{ij}(\mathbf{r}) = \langle v'_i(\mathbf{x})v'_j(\mathbf{x} + \mathbf{r}) \rangle, \quad (1)$$

where $R_{ij}(\mathbf{r})$ is the auto or cross covariance function, $i, j = (1, 2, 3)$ are the indices corresponding to the components of the wind field, \mathbf{x} is the position vector in the three dimensional Cartesian coordinate system, $\mathbf{r} = (r_1, r_2, r_3)$ is the separation vector, $\langle \rangle$ denotes ensemble averaging, and $'$ denotes fluctuations about the ensemble average. Equation (1) denotes a two-point turbulent statistic. At $\mathbf{r} = 0$ we get a single-point turbulent statistic, which we can denote as the variances and covariances. In matrix form it can be written as,

$$\mathbf{R} = \begin{bmatrix} \langle u'^2 \rangle & \langle u'v' \rangle & \langle u'w' \rangle \\ \langle v'u' \rangle & \langle v'^2 \rangle & \langle v'w' \rangle \\ \langle w'u' \rangle & \langle w'v' \rangle & \langle w'^2 \rangle \end{bmatrix}, \quad (2)$$

where the diagonal terms are the variances of the respective wind field components and the off-diagonal terms are the covariances. Here, it is implied that $\mathbf{R} = \mathbf{R}(0)$, and we drop the argument and the bracket for simplicity. From the definition of $\mathbf{R}(\mathbf{r})$ and \mathbf{R} , we can define integral length scale as,

$$l_{ij} = \frac{1}{R_{ij}} \int_0^{\infty} R_{ij}(r_1) dr_1. \quad (3)$$

Lidar turbulence measurements review

A. Sathe and J. Mann

Title Page

Abstract

Introduction

Conclusions

References

Tables

Figures

◀

▶

◀

▶

Back

Close

Full Screen / Esc

Printer-friendly Version

Interactive Discussion



Similar to $R_{ij}(\mathbf{r})$, another useful two-point statistic to characterize turbulence is the velocity structure function, which is defined as,

$$D_{ij}(\mathbf{r}) = \langle (v'_i(\mathbf{x} + \mathbf{r}) - v'_i(\mathbf{x}))(v'_j(\mathbf{x} + \mathbf{r}) - v'_j(\mathbf{x})) \rangle. \quad (4)$$

On many occasions it convenient to study turbulence in the Fourier domain instead of the time domain. To this extent, we can define the spectral velocity tensor (or the three-dimensional spectral density) as the Fourier transform of $R_{ij}(\mathbf{r})$,

$$\Phi_{ij}(\mathbf{k}) = \frac{1}{(2\pi)^3} \int R_{ij}(\mathbf{r}) \exp(i \mathbf{k} \cdot \mathbf{r}) d\mathbf{k}, \quad (5)$$

where $\Phi_{ij}(\mathbf{k})$ is the three-dimensional spectral velocity tensor, $\mathbf{k} = (k_1, k_2, k_3)$ is the wave vector, and $\int d\mathbf{k} = \int_{-\infty}^{\infty} \int_{-\infty}^{\infty} \int_{-\infty}^{\infty} dk_1 dk_2 dk_3$. From Eq. (5) it is obvious that $R_{ij}(\mathbf{r})$ is the inverse Fourier transform of $\Phi_{ij}(\mathbf{k})$. Practically, it is not possible to measure a spectral velocity tensor, since we would need measurements at all points in a three-dimensional space. A one-dimensional velocity spectrum is then used, which is defined as,

$$F_{ij}(k_1) = \frac{1}{2\pi} \int_{-\infty}^{\infty} R_{ij}(r_1) \exp(-ik_1 r_1) dr_1 \quad (6)$$

$$= \int_{-\infty}^{\infty} \int_{-\infty}^{\infty} \Phi_{ij}(\mathbf{k}) dk_2 dk_3. \quad (7)$$

Another important statistic in the Fourier domain is the coherence function defined as,

$$\text{coh}_{ij}(k_1) = \frac{|\chi_{ij}(k_1, r_2, r_3)|^2}{F_{ii}(k_1)F_{jj}(k_1)}, \quad (8)$$

Lidar turbulence measurements review

A. Sathe and J. Mann

Title Page

Abstract

Introduction

Conclusions

References

Tables

Figures

◀

▶

◀

▶

Back

Close

Full Screen / Esc

Printer-friendly Version

Interactive Discussion



where $\chi_{ij}(k_1, r_2, r_3)$ denotes the cross spectra between the components i and j , and $F_{ii}(k_1) = \chi_{ii}(k_1, 0, 0)$, $F_{jj}(k_1) = \chi_{jj}(k_1, 0, 0)$ (no summation over repeated indices) are the one-dimensional spectra of the i and j components respectively.

Ideally, we would like to measure one or more of the quantities in Eqs. (1)–(8) using a lidar. However, owing to inherent difficulties in the lidar systems, quite often it is not possible. We then have to resort to combining lidar measurements with simplified turbulence models that are functions of several variables. As an example, according to Mann (1994), the turbulence structure in the neutral atmospheric surface layer described by $\Phi_{ij}(\mathbf{k})$ can be modeled as a function of only three parameters, $C\varepsilon^{2/3}$, which is a product of the universal Kolmogorov constant $C \approx 1.5$ (Pope, 2000) and the turbulent kinetic energy dissipation rate to the two-third power $\varepsilon^{2/3}$, a characteristic length scale, and an anisotropy parameter. Many studies in the past have attempted to estimate ε from the lidar measurements. Thus, measurement of one or more of the model parameters using lidars is also a significant contribution in the measurement of turbulence.

3 Lidar measurement configurations

A lidar is an acronym for **light detection and ranging**, and some fundamentals of its working can be found in Measures (1984). Most of the past studies have used either of the following three measurement configurations:

1. Staring mode – The lidar beam is fixed at a certain angle with respect to the vertical axis.
2. Scanning mode in a cone – This is called as the **velocity azimuth display** (VAD, also called as the **plan position indicator**, PPI) technique.
3. Scanning mode in a vertical plane – This is called as the **range height indicator** (RHI) scanning technique.

Lidar turbulence measurements review

A. Sathe and J. Mann

Title Page

Abstract

Introduction

Conclusions

References

Tables

Figures

◀

▶

◀

▶

Back

Close

Full Screen / Esc

Printer-friendly Version

Interactive Discussion



3.1 Staring mode

Figure 1 shows the schematic of a lidar operating in a staring mode. At a given instant of time if we assume that a lidar measures at a point, and that the lidar beam is inclined at a certain angle ϕ (in some literature the complement of ϕ is used, which is called as the elevation angle $\alpha = 90^\circ - \phi$) from the vertical axis, and makes an azimuth angle θ with respect to the x_1 axis in the horizontal plane, then the radial velocity (also called as the line-of-sight velocity) can be mathematically written as,

$$v_r(\phi, \theta, d_f) = \mathbf{n}(\phi, \theta) \cdot \mathbf{v}(\mathbf{n}(\phi, \theta)d_f), \quad (9)$$

where v_r is the radial velocity measured at a point, $\mathbf{n} = (\cos\theta \sin\phi, \sin\theta \sin\phi, \cos\phi)$ is the unit directional vector for a given ϕ and θ , and d_f is the distance from the lidar at which the measurement is obtained. In Eq. (9), we have implicitly assumed that v_r is positive for the wind going away from the lidar axis, the coordinate system is right-handed, and u is aligned with the x_1 axis in a horizontal plane. In reality, a lidar never receives backscatter from exactly a point, but from all over the physical space. Fortunately the transverse dimensions of a lidar beam is much smaller than the longitudinal dimensional, and for all practical purposes we can consider that the backscatter is received only along the lidar beam axis. We can then mathematically represent the radial velocity as the convolved signal,

$$\tilde{v}_r(\phi, \theta, d_f) = \int_{-\infty}^{\infty} \varphi(s) \mathbf{n}(\phi, \theta) \cdot \mathbf{v}(\mathbf{n}(\phi, \theta)(d_f + s)) ds, \quad (10)$$

where \tilde{v}_r is the weighted average radial velocity, $\varphi(s)$ is any weighting function integrating to one that depends on the type of lidar, a continuous wave (c-w) lidar or a pulsed lidar, and s is the distance along the beam from the measurement point of interest.

Title Page

Abstract

Introduction

Conclusions

References

Tables

Figures

◀

▶

◀

▶

Back

Close

Full Screen / Esc

Printer-friendly Version

Interactive Discussion



3.2 VAD technique

Figure 2 shows the schematic of the VAD scanning technique. It is an extension of a staring mode, where the lidar beam rotates around a vertical axis, thus forming a cone with the base at the measurement distance of interest and the apex at the lidar source.

v_r is thus measured at different θ and ϕ is kept constant throughout the scan. At a given d_f the radial velocity can be written as,

$$v_r(\theta) = u \cos \theta \sin \phi + v \sin \theta \sin \phi + w \cos \phi. \quad (11)$$

From Eq. (11) we see that when ϕ , θ and d_f are known, v_r is only a function of three unknown wind field components, i.e. u , v and w . In principle, we then need three measurements of \tilde{v}_r at three different θ to deduce the u , v and w components. For a standard VAD scan we normally have much more than three measurements along the azimuth circle. We thus have more equations and only three unknowns, if we assume horizontal homogeneity. Least squares analysis can be used to deduce the three unknown wind field components.

3.3 RHI technique

Figure 3 shows the schematic of the RHI scanning technique. It is also an extension of a staring mode, where the lidar beam rotates in a vertical plane at different ϕ and θ is kept constant throughout the scan. We can use the same Eq. (11) by varying ϕ and keeping θ constant to deduce the wind field components. Actually from a single RHI scan, only two velocity components can be deduced, namely the vertical and the horizontal in the plane of the RHI scan. If $\theta = 0$ is kept constant then the v component cannot be determined (see Eq. 11). Owing to the fact that the lidar is placed on a solid ground, it can only form a semi-circle in a vertical plane. Usually, the scanning plane is aligned such that it is in the mean wind direction. Similar to the VAD technique, if we then have more measurements at different ϕ the three unknown wind field components are estimated using the least squares analysis.

Title Page

Abstract

Introduction

Conclusions

References

Tables

Figures



Back

Close

Full Screen / Esc

Printer-friendly Version

Interactive Discussion



4 State-of-the-art in turbulence measurements using ground-based lidars

Generally, measurement of atmospheric turbulence is a very challenging prospect. With the traditional instruments such as the cup/sonic anemometers, great care has to be taken with regards to sampling frequencies, averaging periods, correction for flow distortions, and orientation of the instrument. When these instruments are properly set up, because they essentially measure at a point, deducing turbulence information from the raw data can be carried out using the standard procedures (Kaimal and Finnigan, 1994). In case of lidars, even if the instrument is correctly set up, due to the fact that they measure in a much larger volume, and at different points in space, standard techniques do not suffice. Deducing turbulence information from the raw lidar data has been and remains the most challenging aspect. In the following sections, at first we discuss the pioneering works that have demonstrated some of the techniques to process the raw lidar data in order to measure turbulence, which is then followed by recent studies that have used some of these techniques.

4.1 Pioneering works

Although much of the lidar turbulence work has been carried out using the scanning configurations described in Sect. 3, the ideas were taken from the pioneering works on radar meteorology (Lhermitte, 1962; Browning and Wexler, 1968). Discussing a bit of mathematics from the radar studies is essential, since they have been and can be used in lidar studies too. Lhermitte (1962) was one of the first to explain the VAD scanning technique using Doppler radars, where v_r is mathematically represented as linear combination of the sine and cosine functions of θ . Browning and Wexler (1968) were the first to conduct an experiment with a pulsed Doppler radar and estimate the u and v components of the wind field along with the mean horizontal divergence, stretching and shearing deformation, in the height range of 1.5–6 km. The latter terms were obtained using a Taylor series expansion around the center of a scanning circle. An error analysis was also carried out to limit the errors in the estimated quantities below a certain

Lidar turbulence measurements review

A. Sathe and J. Mann

Title Page

Abstract

Introduction

Conclusions

References

Tables

Figures



Back

Close

Full Screen / Esc

Printer-friendly Version

Interactive Discussion



level, that led to limiting the values of ϕ . The radar estimated quantities were however not compared with any reference instrument. Based on the VAD scanning, Lhermitte (1969) then suggested a technique of estimating turbulence components R_{ij} that was based on the measurements of the variance of the radial velocity $\langle v_r'^2 \rangle$. Mathematically, by substituting the definition of $n(\phi, \theta)$ into Eq. (11), squaring and ensemble averaging, we get,

$$\langle v_r'^2 \rangle = \langle u'^2 \rangle \sin^2 \phi \cos^2 \theta + \langle v'^2 \rangle \sin^2 \phi \sin^2 \theta + \langle w'^2 \rangle \cos^2 \phi + 2\langle u'v' \rangle \sin^2 \phi \sin \theta \cos \theta + 2\langle u'w' \rangle \sin \phi \cos \phi \cos \theta + 2\langle v'w' \rangle \sin \phi \cos \phi \sin \theta. \quad (12)$$

For ease of reading, we do not include the functional dependence of v_r on ϕ , θ and d_f , but it is implicitly assumed. Wilson (1970) was the first to conduct an experiment using a pulsed Doppler radar and estimate R_{ij} from the $\langle v_r'^2 \rangle$ data in the convective boundary layer (0.1–1.3 km). Only turbulence scales larger than the pulse volume but smaller than the scanning circle could be measured since all the data from a single scan was used. Also, no comparison with any reference instrument was carried out, and hence, the reliability of the radar measurements could not be verified. He demonstrated a mathematically equivalent way of performing the Fourier analysis where integrals were defined in four quadrants as,

$$I_n = \int_{(n-1)\pi/2}^{n\pi/2} \langle v_r'^2 \rangle d\theta, \quad (13)$$

where $n = 1, \dots, 4$. By combining these integrals he then obtained the following expressions,

$$\sin^2 \phi \left(\langle u'^2 \rangle + \langle v'^2 \rangle + \frac{2\langle w'^2 \rangle}{\tan^2 \phi} \right) = \frac{1}{\pi} (I_1 + I_2 + I_3 + I_4), \quad (14)$$

Lidar turbulence measurements review

A. Sathe and J. Mann

Title Page

Abstract

Introduction

Conclusions

References

Tables

Figures

◀

▶

◀

▶

Back

Close

Full Screen / Esc

Printer-friendly Version

Interactive Discussion



Lidar turbulence measurements review

A. Sathe and J. Mann

Title Page

Abstract

Introduction

Conclusions

References

Tables

Figures

◀

▶

◀

▶

Back

Close

Full Screen / Esc

Printer-friendly Version

Interactive Discussion



$$\langle u'w' \rangle \sin 2\phi = \frac{1}{4} \left((I_1 + I_2) - (I_3 + I_4) \right), \quad (15)$$

$$\langle v'w' \rangle \sin 2\phi = \frac{1}{4} \left((I_1 + I_4) - (I_2 + I_3) \right), \quad (16)$$

$$\langle u'v' \rangle \sin^2 \phi = \frac{1}{4} \left((I_1 + I_3) - (I_2 + I_4) \right). \quad (17)$$

5 Using this method we can thus estimate the covariances of \mathbf{R} at a given ϕ . His method was further extended by Kropfli (1986) to include also the turbulence scales larger than the scanning circle by using the data from multiple scans. Although the method was developed for Doppler radar studies, it could also be used for Doppler lidar studies.

10 One of the first lidar studies to measure the u spectrum using a c-w Doppler CO_2 lidar was carried out by Lawrence et al. (1972). The lidar was oriented in the mean wind direction and the measurements were performed at 10 m above the ground, where the probe volume length (also called as the full width half maximum, $\text{FWHM} = 2l$) of the weighting function $\varphi(s)$ was about 30 cm. They concluded that the lidar measurements of the u spectra were considerably better than those obtained using a cup anemometer. In this case $\langle u'^2 \rangle$ can be computed directly from the u fluctuations, since the lidar beam is oriented in the mean wind direction, and the probe volume is quite small. The
 15 aforementioned studies were based on detecting the Doppler shift in the frequency of the reflected radiation. Using a non-Doppler effect technique, Kunkel et al. (1980) was one of the first to estimate $\langle u'^2 \rangle$ using cross-correlation analysis and an aerosol lidar. The lidar beams were scanned in a sequence of three azimuth angles. Turbulence was assumed to be isotropic and the velocity fluctuations were assumed to have a Gaussian distribution. The lidar derived variances compared well with a reference instrument mounted on a tower at 70 m. A technique was also demonstrated to estimate ε from the lidar data, that requires measurements of the boundary layer height z_i , $\langle u'^2 \rangle$ and
 20 the radial velocity spectrum. They estimated z_i using the lidar spectrum observations.

Lidar turbulence measurements review

A. Sathe and J. Mann

Title Page

Abstract

Introduction

Conclusions

References

Tables

Figures

◀

▶

◀

▶

Back

Close

Full Screen / Esc

Printer-friendly Version

Interactive Discussion



As mentioned in Seibert et al. (2000), z_i measurements are subjected to significant uncertainties, and hence, one should be careful in using this method to estimate ε from the lidar data. Hardesty et al. (1982) was one of the first to measure the u spectrum in the rotating plane of a wind turbine of about 20 m diameter. A c-w lidar was placed on a ground and a rotating mirror was mounted on a meteorological tower such that the laser beam directed towards the mirror would focus the beam in a vertical plane at a certain ϕ . Due to the rotating action, VAD scanning was performed in a vertical plane. Taylor series expansion around the center of a scanning circle is then used for the u component, so that the gradients in the vertical and horizontal directions are removed. Owing to the small half-opening angles the contributions by the cross components of R_{ij} were assumed negligible. One has to be careful in using this assumption, as has been explained in detail by Sathe et al. (2011b).

Extending the work of Wilson (1970), Eberhard et al. (1989) derived a new set of equations to estimate R_{ij} from the lidar data using VAD scanning, and they termed their method as the partial Fourier decomposition technique (the same name can also be used for the Wilson, 1970 method). By using standard trigonometric identities, they rearranged Eq. (12) as,

$$\begin{aligned} \langle v_r'^2 \rangle = & \frac{\sin^2 \phi}{2} \left(\langle u'^2 \rangle + \langle v'^2 \rangle + \frac{2\langle w'^2 \rangle}{\tan^2 \phi} \right) + \langle u'w' \rangle \sin 2\phi \cos \theta + \langle v'w' \rangle \sin 2\phi \sin \theta \\ & + \frac{\sin^2 \phi}{2} (\langle u'^2 \rangle - \langle v'^2 \rangle) \cos 2\theta + \langle u'v' \rangle \sin^2 \phi \sin 2\theta. \end{aligned} \quad (18)$$

If we denote Eq. (18) as Fourier series with the corresponding Fourier coefficients, we then have,

$$\frac{\sin^2 \phi}{2} \left(\langle u'^2 \rangle + \langle v'^2 \rangle + \frac{2\langle w'^2 \rangle}{\tan^2 \phi} \right) = \frac{a_0}{2} = \frac{1}{2\pi} \int_0^{2\pi} \langle v_r'^2 \rangle d\theta, \quad (19)$$

Lidar turbulence measurements review

A. Sathe and J. Mann

Title Page

Abstract

Introduction

Conclusions

References

Tables

Figures

◀

▶

◀

▶

Back

Close

Full Screen / Esc

Printer-friendly Version

Interactive Discussion



$$\langle u'w' \rangle \sin 2\phi = a_1 = \frac{1}{\pi} \int_0^{2\pi} \langle v_r'^2 \rangle \cos \theta \, d\theta, \quad (20)$$

$$\langle v'w' \rangle \sin 2\phi = b_1 = \frac{1}{\pi} \int_0^{2\pi} \langle v_r'^2 \rangle \sin \theta \, d\theta, \quad (21)$$

$$\frac{\sin^2 \phi}{2} (\langle u'^2 \rangle - \langle v'^2 \rangle) = a_2 = \frac{1}{\pi} \int_0^{2\pi} \langle v_r'^2 \rangle \cos 2\theta \, d\theta, \quad (22)$$

$$\langle u'v' \rangle \sin^2 \phi = b_2 = \frac{1}{\pi} \int_0^{2\pi} \langle v_r'^2 \rangle \sin 2\theta \, d\theta, \quad (23)$$

where a_0 is the average, a_1 , a_2 are the Fourier cosine, and b_1 , b_2 are the Fourier sine coefficients respectively. As an example, say for a given 30 min time series, if we have several measurements of v_r at each θ , $\langle v_r'^2 \rangle$ can then be computed for each θ , and hence, the corresponding Fourier coefficients. At one half-opening angle, we can thus compute the off-diagonal terms of Eq. (2), i.e. covariances. By measuring at two half-opening angles, and combining Eqs. (19) and (22) we can also compute the variances. As with the Wilson (1970) method, no reference instrument was available to verify the reliability of the measurements. Nevertheless, the study was valuable as the method can potentially be used with the current lidar systems at those sites where the reference measurements are available.

In all of the above studies with a Doppler lidar (or radar), horizontal homogeneity is a key assumption that makes it possible to combine lidar beam measurements from different points in space and obtain turbulence statistics. This limits the application of such studies to only homogeneous flat terrains. Frisch (1991) performed pioneering work on extending the analysis of Wilson (1970) and Eberhard et al. (1989) to also

Lidar turbulence measurements review

A. Sathe and J. Mann

Title Page

Abstract

Introduction

Conclusions

References

Tables

Figures

◀

▶

◀

▶

Back

Close

Full Screen / Esc

Printer-friendly Version

Interactive Discussion



include horizontal inhomogeneities in the turbulence measurements. He demonstrated mathematically that by measuring at three half-opening angles, we can compute R_{ij} using the VAD scanning without assuming horizontal homogeneity. This can potentially have huge implications on turbulence measurements in complex (non-homogeneous) terrain, where wind turbines are subjected to large turbulent forces. Using the Taylor series expansion around the center of a scanning circle, he denoted $\langle v_r'^2 \rangle$ as a Fourier series up to the third harmonic. For each ϕ we then obtain a set of Fourier coefficients, i.e. for $\phi = \phi_1$ we obtain a_{01} as the Fourier coefficient of the zeroth harmonic, a_{11} and b_{11} as the Fourier coefficients of the first harmonic, a_{21}, b_{21} as the Fourier coefficient of the second harmonic, and a_{31} and b_{31} as the Fourier coefficients of the third harmonic. Similarly, we obtain the Fourier coefficients at $\phi = \phi_2$ and $\phi = \phi_3$. The second index in the subscript of the Fourier coefficients denotes the measurement at the corresponding ϕ . To compute R_{ij} , we only need the Fourier coefficients from zeroth up to the second harmonic given by Eqs. (19)–(23). The corresponding expressions for the components of R_{ij} are then given as follows.

$$\langle u'^2 \rangle = t_1 + t_2, \quad (24)$$

$$\langle v'^2 \rangle = t_1 - t_2, \quad (25)$$

where,

Lidar turbulence measurements review

A. Sathe and J. Mann

Title Page

Abstract

Introduction

Conclusions

References

Tables

Figures

◀

▶

◀

▶

Back

Close

Full Screen / Esc

Printer-friendly Version

Interactive Discussion



$$\begin{aligned}
 t_1 = & \left(a_{01} \cos(\phi_3) \left(\sin(\phi_2) \sin(2\phi_2) \cos(\phi_3) - 2 \sin^2(\phi_3) \cos^2(\phi_2) \right) \right. \\
 & + a_{02} \cos(\phi_1) \left(\sin(\phi_3) \sin(2\phi_3) \cos(\phi_1) - 2 \sin^2(\phi_1) \cos^2(\phi_3) \right) \\
 & \left. + a_{03} \cos(\phi_2) \left(\sin(\phi_1) \sin(2\phi_1) \cos(\phi_2) - 2 \sin^2(\phi_2) \cos^2(\phi_1) \right) \right) \\
 & / \left(2 \sin^2(\phi_1) \sin^2(\phi_2) (\cos(\phi_2) - \cos(\phi_1)) \cos^2(\phi_3) \right. \\
 & + 2 \sin^2(\phi_3) (\sin^2(\phi_1) \cos^2(\phi_2) (\cos(\phi_1) - \cos(\phi_3)) \\
 & \left. + \sin^2(\phi_2) \cos^2(\phi_1) (\cos(\phi_3) - \cos(\phi_2))) \right), \\
 t_2 = & \frac{a_{22} \cos(\phi_1) \csc^2(\phi_2) - a_{21} \cos(\phi_2) \csc^2(\phi_1)}{\cos(\phi_1) - \cos(\phi_2)} \quad (26)
 \end{aligned}$$

$$\begin{aligned}
 \langle w'^2 \rangle = & \left(a_{01} \sin^2(\phi_2) \sin^2(\phi_3) (\cos(\phi_2) - \cos(\phi_3)) \right. \\
 & + \sin^2(\phi_1) (a_{02} \sin^2(\phi_3) (\cos(\phi_3) - \cos(\phi_1)) \\
 & \left. + a_{03} \sin^2(\phi_2) (\cos(\phi_1) - \cos(\phi_2))) \right) \\
 & / \left(\sin^2(\phi_1) \sin^2(\phi_2) (\cos(\phi_1) - \cos(\phi_2)) \cos^2(\phi_3) \right. \\
 & + \sin^2(\phi_3) (\sin^2(\phi_1) \cos^2(\phi_2) (\cos(\phi_3) - \cos(\phi_1)) \\
 & \left. + \sin^2(\phi_2) \cos^2(\phi_1) (\cos(\phi_2) - \cos(\phi_3))) \right) \quad (27)
 \end{aligned}$$

$$\langle u'w' \rangle = \frac{a_{11}m_1 + a_{12}m_2 + a_{13}m_3}{\Delta}, \quad (28)$$

$$\langle v'w' \rangle = \frac{b_{11}m_1 + b_{12}m_2 + b_{13}m_3}{\Delta}, \quad (29)$$

where,

$$\begin{aligned} m_1 &= \sin(\phi_2) \sin(\phi_3) (\cos(2\phi_3) - \cos(2\phi_2)), \\ m_2 &= \frac{1}{2} (\sin(3\phi_1) \sin(\phi_3) - \sin(\phi_1) \sin(3\phi_3)), \\ m_3 &= \sin(\phi_1) \sin(\phi_2) (\cos(2\phi_2) - \cos(2\phi_1)), \\ \Delta &= 2 \sin^3(\phi_3) \left(\sin(\phi_1) \sin(2\phi_2) \cos^2(\phi_1) - \sin(2\phi_1) \sin(\phi_2) \cos^2(\phi_2) \right) \\ &\quad + 2 \left(\sin(2\phi_1) \sin^3(\phi_2) - \sin^3(\phi_1) \sin(2\phi_2) \right) \sin(\phi_3) \cos^2(\phi_3) \\ &\quad + \sin(\phi_1) \sin(\phi_2) \sin(2\phi_3) (\cos(2\phi_2) - \cos(2\phi_1)). \end{aligned} \quad (30)$$

$$\langle u'v' \rangle = \frac{b_{22} \cos(\phi_1) \csc^2(\phi_2) - b_{21} \cos(\phi_2) \csc^2(\phi_1)}{\cos(\phi_1) - \cos(\phi_2)} \quad (31)$$

Unfortunately, not much information is given regarding any experimental study, and hence, the validity and reliability of this technique remains unknown. Nevertheless, the technique remains a potential solution to measure turbulence in complex terrain. Using a different scanning strategy, Gal-Chen et al. (1992) was one of the first to employ RHI scanning to estimate R_{ij} . They used a pulsed CO₂ Doppler lidar in the mean wind direction and perpendicular to the mean wind direction. The equations for $\langle v_r'^2 \rangle$ are given as,

$$\langle v_r'^2 \rangle = \langle u'^2 \rangle \sin^2 \phi + \langle w'^2 \rangle \cos^2 \phi \pm \langle u'w' \rangle \sin(2\phi), \quad (32)$$

Lidar turbulence measurements review

A. Sathe and J. Mann

Title Page	
Abstract	Introduction
Conclusions	References
Tables	Figures
◀	▶
◀	▶
Back	Close
Full Screen / Esc	
Printer-friendly Version	
Interactive Discussion	



for the lidar beam aligned in the mean wind direction. The \pm sign for $\langle u'w' \rangle$ depends on whether the wind is blowing away from or towards the lidar beam. Similarly, for the cross wind direction we have,

$$\langle v_r'^2 \rangle = \langle v'^2 \rangle \sin^2 \phi + \langle w'^2 \rangle \cos^2 \phi \pm \langle v'w' \rangle \sin(2\phi), \quad (33)$$

5 where the \pm sign depends on positive and negative cross wind beam direction. Equations (32) and (33) are then solved using the least squares analysis to obtain components of R_{ij} (except $\langle u'v' \rangle$). A method to estimate ε is also provided using the one-dimensional longitudinal spectrum. In the inertial subrange, the following relation is known (Pope, 2000).

$$10 \quad F_{11}(k_1) = C_1 \varepsilon^{2/3} k_1^{-5/3}, \quad (34)$$

where $F_{11}(k_1)$ is the one-dimensional spectrum of the longitudinal wind field component, and $C_1 \approx 0.5$ is the Kolmogorov constant related to $F_{11}(k_1)$. The spectrum is measured using a lidar at low elevation angle, and the inertial range can be established by fitting the $-5/3$ slope to the spectrum measurements. ε can then be estimated using
 15 Eq. (34) provided that the averaging is taken care of or can be ignored. An innovative method was also provided to compute the surface heat flux using the third moment of the vertical velocity by the following equation,

$$\frac{\partial}{\partial z} \left(\frac{1}{2} \langle w'^3 \rangle \right) = \frac{1}{\rho} \langle w' \frac{\partial p'}{\partial z} \rangle - \frac{\varepsilon}{3} + \frac{g}{\theta_T} \langle w' \theta'_T \rangle, \quad (35)$$

where $\langle w'^3 \rangle$ is the third moment of the vertical velocity, z is the height above the ground,
 20 $\partial/\partial z$ is the vertical gradient, p' is the pressure fluctuation, ρ is the air density at the surface, θ_T is the surface potential temperature, and $\langle w' \theta'_T \rangle$ is the sensible heat flux. Wyngaard and Coté (1971) showed that the pressure covariance term at the surface is negligible, and thus can be neglected in the surface measurements. $\langle w'^3 \rangle$ can be

Lidar turbulence measurements review

A. Sathe and J. Mann

Title Page	
Abstract	Introduction
Conclusions	References
Tables	Figures
◀	▶
◀	▶
Back	Close
Full Screen / Esc	
Printer-friendly Version	
Interactive Discussion	



Lidar turbulence measurements review

A. Sathe and J. Mann

Title Page

Abstract

Introduction

Conclusions

References

Tables

Figures

◀

▶

◀

▶

Back

Close

Full Screen / Esc

Printer-friendly Version

Interactive Discussion



measured using lidar measurements, and hence, $\langle w'\theta' \rangle$ can be measured indirectly using Eq. (35). It should be noted that the averaging time required for the third moments are significantly larger than those required to compute the lower order moments, owing to its influence on the systematic and random errors (Lenschow et al., 1994). Again, owing to the measurement heights of interest, no reference instrument was available, and hence, the reliability of lidar measurements is unknown. It should also be noted that at small elevation angles, the assumption of horizontal homogeneity may not be valid, and one has to take this into account while interpreting the lidar measurements.

In all of the above studies with a Doppler lidar (or radar), the estimated turbulence statistics from the lidar measurements will be subjected to different levels of volume averaging errors, depending on the type of lidar, c-w or pulsed, height above the ground, and the turbulence structure in the atmosphere (Sathe et al., 2011b). None of the aforementioned studies have attempted to correct the turbulence statistics for the errors due to finite probe volume of a lidar, possibly because many were interested to measure in the convective boundary layer. In this layer the turbulence scales are quite large (Wynngaard, 2010), and perhaps probe volume averaging does not matter. However, if the measurements are desired closer to the ground, particularly in the first 200 m above the ground where the wind turbines operate, then one must account for the averaging effects in the probe volume. Frehlich (1994) and Frehlich et al. (1994) demonstrated this averaging effect in the measurement of the structure function, where for smaller separation distances the averaging effect was more pronounced. Smalikho (1995) was the first to derive explicit formulae to account for the small scale filtering effect of the finite probe volume for a c-w lidar. The formulae for the estimation of ε were derived using three different methods for a staring lidar, i.e. using

- the width of the Doppler spectrum,
- the velocity structure function, and
- the one-dimensional velocity spectrum.

He derived the following expression for the width of the Doppler spectrum,

$$\langle \sigma_s^2 \rangle = 1.22C\varepsilon^{2/3}l^{2/3}, \quad (36)$$

where $\langle \sigma_s^2 \rangle$ is the second central moment of the Doppler spectrum (or its width), and l is the Rayleigh length (which for a c-w lidar is the same as the half width half maximum of the weighting function of the probe volume). It should be noted that there is a slight difference in the value of the Kolmogorov constant used in Banakh et al. (1999), although the same Eq. (36) is stated also in Smalikho (1995), i.e. in Eq. (25) of Smalikho (1995) the value of Kolmogorov constant is ≈ 1.83 , whereas in Eq. (13) of Banakh et al. (1999), the value of Kolmogorov constant is ≈ 2 . For a continuous wave lidar $\varphi(s)$ is well approximated by a Lorentzian function (Sonnenschein and Horrigan, 1971), and $l = \lambda_b d_f^2 / \pi r_b^2$, where λ_b is the wavelength of the emitted radiation, and r_b is the beam radius. $\langle \sigma_s^2 \rangle$ can be measured, l is known, so ε can be estimated. The limitations of this method is that Eq. (36) can only be used when $l \ll \mathcal{L}$, where \mathcal{L} is the outer scale of turbulence. Moreover the effect of mean radial velocity gradient within the probe volume has not been taken into account. Equation (36) says that if there is no turbulence then the Doppler spectral width should be zero. However if there is a mean change of v_r with s (within the probe volume) then there is an additional term proportional to l^2 . If the lidar is c-w and the shear is linear then the coefficient of l^2 is infinite (Mann et al., 2010) and we cannot use this method.

The expression for the structure function was derived using the assumption of local isotropy in the inertial subrange. Kristensen et al. (2011) re-derived the expression in great detail, where the probe volume weighting function is assumed be Lorentzian. The expression is given as,

$$\tilde{D}(r_1) = C\varepsilon^{2/3}l^{2/3} \frac{\Gamma(1/3)}{5\sqrt{\pi}\Gamma(5/6)} \int_0^{2\pi} \left(1 - \frac{8}{11} \cos^2 \xi\right) \Psi(r_1, \Theta, \xi) d\xi, \quad (37)$$

Lidar turbulence measurements review

A. Sathe and J. Mann

Title Page

Abstract

Introduction

Conclusions

References

Tables

Figures

◀

▶

◀

▶

Back

Close

Full Screen / Esc

Printer-friendly Version

Interactive Discussion



where $\tilde{D}(r_1)$ is the filtered radial velocity structure function measured by the lidar, $r_1 = \langle u \rangle t$ is the separation distance along the x_1 axis, $\Gamma(n) = \int_0^\infty x^{n-1} \exp(-x) dx$ is the gamma function, Θ is the angle between the lidar beam and the mean wind $\langle u \rangle$, and

$$\Psi(r_1, \Theta, \xi) = \frac{3}{2} \Gamma\left(\frac{1}{3}\right) \left(\left(\cos^2 \xi + \left(\frac{r_1}{l}\right)^2 \cos^2(\xi + \Theta) \right)^{1/3} \cdot \cos\left(\frac{2}{3} \tan^{-1}\left(\frac{r_1}{l} \left| \frac{\cos(\xi + \Theta)}{\cos \xi} \right| \right)\right) - |\cos \xi|^{2/3} \right). \quad (38)$$

r_1 is computed using the Taylor's hypothesis (Taylor, 1938), where turbulence is assumed to be advected by the mean wind $\langle u \rangle$ in time t . For the measured and known parameters $\tilde{D}(r_1)$, r_1 , l and C , the unknown ε can be estimated, where the one-dimensional integral in Eq. (37) can be solved numerically. Using similar approach the expressions for the one-dimensional velocity spectrum are also derived by Smalikho (1995) and Kristensen et al. (2011). However, due to the equivalence of the structure function and spectrum approach, the expressions for the same are not explicitly stated here.

The limitation of the structure function approach using a staring Doppler lidar is that if there is little or no mean wind then Taylor's hypothesis is violated and the structure functions cannot be estimated. In order to counter these limitations Banakh et al. (1996) proposed a novel technique to estimate ε using the VAD scanning. Instead of measuring the structure function based on a separation distance r_1 and using the Taylor's hypothesis, it is measured based on an angular separation distance $d_f \delta$ on the base of the scanning cone, where $\delta = 2 \sin^{-1}(\sin \phi \sin \theta)$ is the angle subtended by the two lidar beams in a VAD scanning. There is however an assumption that the scanning speed is much larger than the advection speed of the turbulence. Kristensen et al. (2012) re-derived the expressions using this approach but neglected the contribution due to random instrumental noise that was considered in Banakh et al. (1996). For modern lidar systems the instrumental noise can be neglected (Mann et al., 2009), but for older systems was found significant (Frehlich et al., 1998; Drobinski et al., 2000),

Lidar turbulence measurements review

A. Sathe and J. Mann

Title Page

Abstract

Introduction

Conclusions

References

Tables

Figures



Back

Close

Full Screen / Esc

Printer-friendly Version

Interactive Discussion



and hence, one must be careful before neglecting it. Two approaches were chosen in the derivation by Kristensen et al. (2012); time domain autocorrelation approach, and the Fourier domain wave-number approach. The Fourier domain approach is derived for a c-w lidar (assuming a Lorentzian function), whereas the time domain approach provides expressions as a function of $\varphi(s)$. By using appropriate $\varphi(s)$, the time domain expressions can be applied for a c-w or a pulsed lidar. The equations using both approaches are as follows. In the time domain,

$$\begin{aligned} \tilde{D}(\delta) = & 2(1 - \cos \delta)R(0) + \frac{9}{55}\Gamma\left(\frac{1}{3}\right)C(\varepsilon d_f)^{2/3} \int_{-\infty}^{\infty} \int_{-\infty}^{\infty} \varphi(s'_1)\varphi(s'_2) \\ & \cdot \left(3 \left((s'_2 - s'_1)^2 + 4s'_1 s'_2 \sin^2(\delta/2) \right)^{1/3} \cos \delta - |s'_2 - s'_1|^{2/3} \right) \\ & + \frac{s'_1 s'_2 \sin^2 \delta}{((s'_2 - s'_1)^2 + 4s'_1 s'_2 \sin^2(\delta/2))^{2/3}} \Big) ds'_1 ds'_2, \end{aligned} \quad (39)$$

where $\tilde{D}(\delta)$ is the filtered radial velocity structure function for a separation distance $d_f \delta$ on the base of the cone, $R(0) = \langle u'^2 \rangle = \langle v'^2 \rangle = \langle w'^2 \rangle$ for isotropic turbulence, and $s'_1 = s_1/d_f$, $s'_2 = s_2/d_f$ are non-dimensional variables. In the Fourier domain, for a c-w lidar,

Lidar turbulence measurements review

A. Sathe and J. Mann

Title Page

Abstract

Introduction

Conclusions

References

Tables

Figures



Back

Close

Full Screen / Esc

Printer-friendly Version

Interactive Discussion



Lidar turbulence measurements review

A. Sathe and J. Mann

Title Page

Abstract

Introduction

Conclusions

References

Tables

Figures

◀

▶

◀

▶

Back

Close

Full Screen / Esc

Printer-friendly Version

Interactive Discussion



$$\begin{aligned}
 \tilde{D}(\delta) = & 2(1 - \cos \delta)R(0) + C(\varepsilon d_f)^{2/3} \frac{3}{55} \Gamma\left(\frac{1}{3}\right) \\
 & \cdot \left(\frac{3}{\sqrt[3]{2}} (1 + 7 \cos \delta) \sin^{2/3}(\delta/2) - 18 \left(\frac{d_f}{l}\right)^{-2/3} \right. \\
 & + \frac{1}{\pi} \left(\frac{2d_f}{l}\right)^{-2/3} \int_0^{\pi/2} \frac{\Gamma(1/2)\Gamma(1/3)}{\Gamma(5/6)} (7 \cos \delta - 4 \cos(2\xi)) \\
 & \cdot \left(2 \cos\left(\frac{2}{3} \tan^{-1}\left(\frac{4d_f \sin(\delta/2) \sin \xi}{l(|\cos(\xi + \delta/2)| + |\cos(\xi - \delta/2)|)}\right)\right) \right) \\
 & \cdot \left((|\cos(\xi + \delta/2)| + |\cos(\xi - \delta/2)|)^2 + 16 \left(\frac{d_f}{l}\right)^2 \sin^2(\delta/2) \sin^2 \xi \right)^{1/3} \\
 & - \left(4 \frac{d_f}{l} \sin(\delta/2) \sin \xi \right)^{2/3} \Big) d\xi. \tag{40}
 \end{aligned}$$

As in the Smalikho (1995) method, the key to using this method is to appropriately select $d_f \delta \ll \mathcal{L}$, so that turbulence is measured in the inertial subrange, and is locally isotropic. $D(\delta)$ can be measured using a lidar, then by knowing $R(0)$, we can estimate ε . Banakh et al. (1996) did not include the $R(0)$ term in their equation, perhaps because at $\delta \ll \pi/2$, and $d_f \gg \mathcal{L}$, this term is negligible. The advantage of using Eq. (40) is that we need to solve only a single integral numerically, whereas in Eq. (39) we need to solve a double integral numerically, that may increase the numerical error. The estimation of $R(0)$ can be quite challenging, since it also contains information of the large scale turbulence. Kristensen et al. (2012) used empirical models for convective turbulence (Kristensen et al., 1989) and estimated $R(0) = 1.74 \varepsilon^{2/3} (d_f \cos \phi)^{2/3}$. Alternatively one may use the von Kármán (1948) energy spectrum and derive expressions for $R(0)$. The experimental verification of the Kristensen et al. (2011, 2012) expressions remains to

be seen, but that using the Smalikho (1995) and Banakh et al. (1996) expressions will be discussed later in the article.

One of the biggest limitations of a c-w lidar is that $I \propto d_f^2$, and hence, measuring at greater heights becomes a problem owing to the large probe volume. A pulsed lidar is then ideally suited for this purpose since the length of the probe volume remains constant at all heights. To this extent, Frehlich (1997) was one of the first to derive expressions for the filtered velocity correlation and structure function measured by a pulsed lidar. Numerical simulations were performed to verify the model, where close agreement was observed. The covariances and structure functions of the radial velocities are expressed as a function of lidar parameters and single point statistics. If we define the range gate length of a pulsed lidar as $L_p = c\tau/2$, where c is the speed of light, and τ is the pulse duration, then he derived the following equation for the filtered covariance function of the radial velocity,

$$\tilde{R}(r) = \langle v_r'^2 \rangle \int_{-\infty}^{\infty} f(x, \mu) (1 - \Lambda(\chi|y - x|)) dx, \quad (41)$$

where r is the separation distance along the beam, $y = r/L_p$, $\mu = \sqrt{2 \ln(2)} L_p / l$, $\chi = L_p / \mathcal{L}$,

$$\Lambda(x) = (ax)^{2/3} (1 + (ax)^b)^{-2/3b}, \quad (42)$$

is supposedly the normalized structure function of the radial velocity component, and

$$f(x, \mu) = \frac{1}{2\sqrt{\pi}\mu} \left(\exp(-\mu^2(x+1)^2) + \exp(-\mu^2(x-1)^2) \right) + \frac{x}{2} \left(\operatorname{erf}(\mu(x+1)) + \operatorname{erf}(\mu(x-1)) - 2\operatorname{erf}(\mu x) \right) - \frac{1}{\sqrt{\pi}\mu} \exp(-\mu^2 x^2) + \frac{\operatorname{erf}(\mu(x+1))}{2} - \frac{\operatorname{erf}(\mu(x-1))}{2}, \quad (43)$$

Lidar turbulence measurements review

A. Sathe and J. Mann

Title Page

Abstract

Introduction

Conclusions

References

Tables

Figures

◀

▶

◀

▶

Back

Close

Full Screen / Esc

Printer-friendly Version

Interactive Discussion



Lidar turbulence measurements review

A. Sathe and J. Mann

Title Page

Abstract

Introduction

Conclusions

References

Tables

Figures

◀

▶

◀

▶

Back

Close

Full Screen / Esc

Printer-friendly Version

Interactive Discussion



where $f(x, \mu)$ is the filter function for a Gaussian transmitted pulse and a rectangular time window. Frehlich (1997) mentions that Eq. (42) is the universal function given by Kaimal et al. (1972), but we could not verify that, where for neutral conditions, $a = 0.26278$ and $b = 1.1948$, and $\text{erf}(x) = 2/\sqrt{\pi} \int_0^x \exp(-t^2) dt$ is the error function. In order to use Eq. (41) it is necessary that $r \ll \mathcal{L}$. The filtered radial velocity structure function is given as,

$$\tilde{D}(r) = 2\langle v_r'^2 \rangle \int_{-\infty}^{\infty} f(x, \mu) (\Lambda(x|y-x) - \Lambda(x|x)) dx. \quad (44)$$

In both Eqs. (41) and (44) an empirical $\Lambda(x)$ function is used to express $\tilde{R}(r)$ and $\tilde{D}(r)$ in terms of $\langle v_r'^2 \rangle$ and \mathcal{L} , but in principle we could also use the von Kármán (1948) model. By measuring $\tilde{R}(r)$ or $\tilde{D}(r)$ using a lidar, \mathcal{L} and $\langle v_r'^2 \rangle$ can be obtained by the fitting the measurements to Eqs. (41) or (44). Having obtained $\langle v_r'^2 \rangle$, any/all of the Eqs. (13)–(33) can be used to estimate R_{ij} .

In an independent study, Banakh and Smalikho (1997b) also derived expressions for the estimation of ε using a staring pulsed lidar. They followed the same structure function approach as in Smalikho (1995). Using numerical simulation they compared the performance of their model with the numerical results, and concluded that the relative errors in the estimation of ε are between 15–20% for a signal-to-noise ratio equal to or greater than unity. Comparison of the model with the measurements will be more challenging, and possibly provide more confidence in the method. As for the c-w lidar, Kristensen et al. (2011) re-derived the expressions in great detail. As with Frehlich (1997) they also assumed a Gaussian transmitting pulse. If we define w_p as the pulse width then Kristensen et al. (2011) introduced a length scale $l_p = \sqrt{L_p^2/12 + w_p^2}$ and used the same same expression as Eq. (37) also for the pulsed lidar, except that l in Eq. (37) is replaced by l_p and the $\Psi(r_1, \Theta, \xi)$ function is now given as,

Lidar turbulence measurements review

A. Sathe and J. Mann

Title Page

Abstract

Introduction

Conclusions

References

Tables

Figures

◀

▶

◀

▶

Back

Close

Full Screen / Esc

Printer-friendly Version

Interactive Discussion



$$\Psi(r_1, \Theta, \xi) = \frac{3}{2} \Gamma\left(\frac{2}{3}\right) |\cos \xi|^{2/3} \left({}_1F_1\left(-\frac{1}{3}; \frac{1}{2}; -\frac{r_1^2 \cos^2(\xi + \Theta)}{4l_p^2 \cos^2 \xi}\right) - 1 \right), \quad (45)$$

where ${}_1F_1(a; b; x)$ is the Kummer confluent hypergeometric function (Abramowitz and Stegun, 1965). It is to be noted that using Eqs. (37) and (45), for some combinations of α and r_1/l (or r_1/l_p), $\tilde{D}(r_1)$ becomes negative, but Kristensen et al. (2011) also provide the range within which Eqs. (37) and (45) are valid. An advantage of using a pulsed lidar is also that we do not need to apply Taylor's hypothesis in order to compute the separation distance. Thus instead of using r_1 in Eq. (45) we can use the separation distance r (provided that $r \ll \mathcal{L}$) along the lidar beam, since a pulsed lidar measures at different range gates simultaneously, and hence measure $\tilde{D}(r)$ along the lidar beam axis (Frehlich, 1997).

For a c-w lidar, it is reasonable to assume that the Doppler spectrum obtains its width mainly due to velocity variations (and perhaps also the mean shear) inside the probe length of the lidar. For a pulsed lidar, this assumption is not reasonable, since some lidar parameters like the finite pulse width also contributes to the width of the Doppler spectra. Extracting turbulence information from the width of a Doppler spectra for a pulsed lidar is then much more challenging. Nevertheless, Smalikho et al. (2005) demonstrated that by depicting the Doppler spectral width as a linear summation of contributions from atmospheric turbulence and lidar parameters, we can successfully measure ε . Using numerical simulations they concluded that the bias in ε is very sensitive to the selection of the optimal noise threshold level. Interestingly they compared the estimations of ε obtained by the spectral width approach and those obtained by the structure function approach (Frehlich, 1997; Banakh and Smalikho, 1997b), and concluded that at low turbulence levels, the structure function approach results in lower random errors of ε , whereas at higher turbulence levels, the random errors in ε obtained by the spectral width approach are two times smaller than those obtained by the structure function approach. The experiment was carried out using the RHI scanning,

but since no reference instruments were available, the reliability of this technique was unknown.

From the above it can be seen that the major works on processing raw lidar data and obtaining unfiltered turbulence parameters are based on the filtered radial velocity covariances and structure functions. In all these works, the filter function is obtained by assuming either the isotropy of turbulence in the inertial sub-range or the entire range of turbulence scales. It is however well-known that turbulence is not isotropic on all scales of interest (Kaimal et al., 1972; Mann, 1994). Hence, $\langle v_r'^2 \rangle$ and \mathcal{L} obtained by fitting the modeled structure function to the measurements (Frehlich et al., 1998) is not entirely reliable. A better solution would then be to use anisotropic turbulence model (Mann, 1994) in modeling the structure function measured by the lidar, and then fitting it to the measurements (Frehlich et al., 2006; Frehlich and Kelley, 2008). Even using an anisotropic turbulence model may not provide reliable estimates of turbulence statistics under all conditions, e.g. Mann (1994) model is strictly valid only for homogeneous neutral surface layer. Alternatively, it would be best if we do not need to combine turbulence models with measurements, so that we get more reliable statistics from lidar measurements. Mann et al. (2010) provided one such technique to obtain unfiltered radial velocity variance for a c-w lidar without using any turbulence models. They suggested using the mean Doppler spectra given as,

$$\langle S(v_r) \rangle = \frac{f(\eta) + f(\eta^*)}{\sqrt{8\pi\langle v_r'^2 \rangle}}, \quad (46)$$

where $\eta = (G + iv_r)/\sqrt{2\langle v_r'^2 \rangle}$, G is the mean radial velocity gradient, $*$ denotes complex conjugation, and $f(\eta) = \exp(\eta^2)(1 - \text{erf } \eta)$. They assumed that the probability density function of v_r at a given position s inside the probe volume is Gaussian distributed, and that $\langle v_r'^2 \rangle$ is constant inside the probe volume. A systematic study of the influence of these assumptions on the turbulence statistics has however not been carried out. By fitting Eq. (46) to measurements of $\langle S(v_r) \rangle$, $\langle v_r'^2 \rangle$ can be estimated.

Lidar turbulence measurements review

A. Sathe and J. Mann

Title Page

Abstract

Introduction

Conclusions

References

Tables

Figures

◀

▶

◀

▶

Back

Close

Full Screen / Esc

Printer-friendly Version

Interactive Discussion



4.2 Classification of the previous works according to the estimated turbulence quantity

From the previous section it can well be understood that processing raw lidar signals to extract turbulence information is an extremely challenging task. Up until the mid and late 1990s, focus was more into developing new data processing methods to extract turbulence information. New algorithms for efficiently processing the raw lidar data are still being developed as seen in the recent work by Mann et al. (2010). Nevertheless, many studies have benefited from the continuous developments in the past, where simulation studies and measurement campaigns have been carried out. Because lidar is not yet an established technology to measure atmospheric turbulence, it is important to compare lidar measurements with a reference instrument, as emphasised in the review article by Wilczak et al. (1996). In their review, lidar technology was termed to be a “young adult” in comparison to sodars and radars. With the recent spurt in the measurement campaigns using lidars, we think that it has grown beyond its status of “young adult”.

Table 1 groups the studies that have focused on estimation of turbulence quantities using either simulation or lidar measurements. For each turbulence quantity, the total number of studies is also given. It is evident that significant efforts have been focused on estimation of ε , followed by R_{ij} , ℓ_{ij} , $\langle v_r'^2 \rangle$, $\tilde{D}(r)$, $\tilde{F}(k_1)$, and $F_{ij}(k_1)$.

4.2.1 ε , $\tilde{F}(k_1)$, $\tilde{D}(r)$

The greatest advantage of estimation of ε is that we can exploit the universal behaviour of isotropy in the inertial subrange, either in the Fourier domain (using velocity spectrum) or the temporal domain (using structure function) (Pope, 2000). Thus estimation of ε involves estimation of either $\tilde{F}(k_1)$ or $\tilde{D}(r)$ (we could also use the separation distance r_1 instead of r) in the inertial subrange from the lidar beam that is oriented in any direction. The challenges associated are then threefold; existence of the inertial subrange, identification of the inertial subrange from the lidar data, and probe volume

Lidar turbulence measurements review

A. Sathe and J. Mann

Title Page

Abstract

Introduction

Conclusions

References

Tables

Figures

◀

▶

◀

▶

Back

Close

Full Screen / Esc

Printer-friendly Version

Interactive Discussion



Lidar turbulence measurements review

A. Sathe and J. Mann

Title Page

Abstract

Introduction

Conclusions

References

Tables

Figures

◀

▶

◀

▶

Back

Close

Full Screen / Esc

Printer-friendly Version

Interactive Discussion



averaging. From Pope (2000) we understand that in order to have a well defined inertial subrange, we need large Reynolds number flows. Fortunately, atmospheric flows are usually characterized by large Reynolds number (Wyngaard, 2010), especially during convective day-time conditions. Stable atmospheric conditions that normally occur during late night and early morning, can however present challenges since they are associated with low Reynolds number turbulence (Wyngaard, 2010). We can then assume that inertial subrange is well defined for most part of the day, except during late night and early morning conditions.

The challenge associated with identifying the inertial subrange from lidar measurements is mainly due to the probe length of a lidar. In principle we need only one measurement of either $\tilde{F}(k_1)$ or $\tilde{D}(r)$ in the inertial subrange. However, in order to avoid statistical uncertainty, it is recommended to have more measurements, and thus fit a model to the measurements. From Mann et al. (2009), Sjöholm et al. (2009) and Sathe (2012), it is clear that due to the probe length of a lidar, most of the turbulence scales in the inertial range are filtered out. Modeling the lidar filter function then becomes inevitable, which has fortunately been carried out by Smalikho (1995), Banakh et al. (1996), Frehlich (1997), Smalikho et al. (2005), Sjöholm et al. (2009) and Mann et al. (2009). In Sjöholm et al. (2009) and Mann et al. (2009), the goal was only to compare the lidar volume averaged measurements of the radial velocity spectrum with reference point measurements, and estimation of ε is not carried out. These studies could be extended further to estimate ε by using the isotropic or anisotropic form of spectral tensor with a given energy spectrum. Apart from the filtering effect, we also need to identify the cut-off low wavenumber range in case of $\tilde{F}(k_1)$, and the maximum separation distance in case of $\tilde{D}(r)$, to identify the inertial subrange.

In summary, there are four ways of estimating ε ; width of the Doppler spectra (Smalikho, 1995; Banakh et al., 1995a, 2010; Smalikho et al., 2005), radial velocity spectrum (Gal-Chen et al., 1992; Banakh et al., 1995b, 1997; Banakh and Smalikho, 1997a; Drobinski et al., 2000; Davies et al., 2005; Davis et al., 2008; Collier et al., 2005; Lothon et al., 2009; O'Connor et al., 2010; Dors et al., 2011; Kristensen et al., 2011),

Lidar turbulence measurements review

A. Sathe and J. Mann

Title Page

Abstract

Introduction

Conclusions

References

Tables

Figures



Back

Close

Full Screen / Esc

Printer-friendly Version

Interactive Discussion



line-of-sight radial velocity structure function (Frehlich et al., 1994; Frehlich, 1997; Banakh and Smalikho, 1997a,b; Frehlich et al., 1998; Banakh et al., 1999; Frehlich and Cornman, 2002; Davies et al., 2004; Banakh and Werner, 2005; Smalikho et al., 2005), and radial velocity azimuthal structure function (Banakh et al., 1996, 1999; Banakh and Smalikho, 1997a; Frehlich et al., 2006, 2008; Frehlich and Kelley, 2008; Chan, 2011; Kristensen et al., 2012). Very few studies have exploited the Doppler spectral width to estimate ε , where the reasons could be that for a c-w lidar its applicability is limited to $l \ll \mathcal{L}$, and for a pulsed lidar it is quite complicated to process the data (Smalikho et al., 2005). Nevertheless, as shown by Banakh et al. (2010), for a pulsed lidar it could be advantageous to use the Doppler spectral width approach, since the random errors in ε can be reduced at higher turbulence levels in comparison to using the structure function approach, or equivalently using the radial velocity spectrum approach.

4.2.2 $\langle v_r'^2 \rangle$, ℓ_{ij} , \mathcal{L}

Apart from ε , another important parameter that characterizes turbulence is the length scale. The two most commonly used definitions of the length scale are ℓ_{ij} and \mathcal{L} , which have physically different interpretations. \mathcal{L} (also called as the outer length scale of turbulence) is the length scale corresponding to the maximum spectral energy, whereas ℓ_{ij} can be interpreted as the length scale up to which turbulence is correlated. They can however be shown to be related to each other, as done by Frehlich and Cornman (2002), Smalikho et al. (2005) and Lothon et al. (2006). Thus ℓ_{ij} can be estimated using the relationship with \mathcal{L} (Frehlich and Cornman, 2002; Davies et al., 2004; Collier et al., 2005; Smalikho et al., 2005; Lothon et al., 2006, 2009; Frehlich et al., 2006), or by using the definition given by Eq. (3) (Cohn et al., 1998). Practically ℓ_{ij} is estimated from the values of autocorrelation function at the first zero crossing, but Davies et al. (2005) estimated the same using some properties of the autocorrelation function. \mathcal{L} can be estimated using the structure function approach (Frehlich, 1997; Frehlich et al., 1998, 2008; Frehlich and Kelley, 2008). Drobinski et al. (2000) followed a slightly different approach, where the radial velocity spectrum is split into two regions, one is the energy

Lidar turbulence measurements review

A. Sathe and J. Mann

Title Page

Abstract

Introduction

Conclusions

References

Tables

Figures

◀

▶

◀

▶

Back

Close

Full Screen / Esc

Printer-friendly Version

Interactive Discussion



containing range, and the other containing the inertial subrange up to the dissipation range. Measurements of the radial velocity spectrum can thus be fitted to this model and \mathcal{L} , ε estimated simultaneously. Interestingly Banakh et al. (1999) and Banakh and Werner (2005) use the term outer length scale also for ℓ_{ij} , but we believe that it is important to distinguish between the two length scales.

Compared to ε , fewer studies have been carried out to estimate $\langle v_r'^2 \rangle$ (see Table 1). It is perhaps because of the information of all turbulence scales that is required to estimate $\langle v_r'^2 \rangle$, and a universal isotropic relation does not suffice. Although Eberhard et al. (1989); Gal-Chen et al. (1992) have estimated $\langle v_r'^2 \rangle$ from lidar measurements, no consideration to probe volume averaging was given, and thus any other turbulence statistic derived using these measurements would not contain information of small scale turbulence. All subsequent studies have followed the pioneering work of Frehlich (1997), where information of small scale turbulence was recovered by modelling the filter function. The main contribution of the Frehlich (1997) method is that it presents a technique to derive expressions of the radial velocity structure function (or equivalently the radial velocity spectrum) for any given shape of the lidar pulse and a turbulence model, with which we can estimate $\langle v_r'^2 \rangle$ and ℓ_{ij} . One can thus use a non-Gaussian shape of the pulse and derive a different functional form of the spatial filter (Davies et al., 2004), or use a different turbulence model, e.g. von Kármán (1948) isotropic spectral tensor model (Frehlich and Cornman, 2002), or a more realistic anisotropic Mann (1994) spectral tensor instead of the empirical Kaimal et al. (1972) models (Frehlich, 1997; Frehlich et al., 1998). Using $\tilde{D}(r)$ to estimate $\langle v_r'^2 \rangle$ from a pulsed lidar has the limitation of coarse vertical resolution. An azimuthal structure function approach can then be used to improve the vertical resolution (Banakh et al., 1996; Frehlich et al., 2006; Frehlich and Kelley, 2008; Kristensen et al., 2012). Without using any turbulence model, Mann et al. (2010) suggested a technique (only for c-w lidars) to estimate $\langle v_r'^2 \rangle$ using the mean Doppler spectrum. The validity of this technique is successfully demonstrated in Branstard et al. (2013).

4.2.3 $R_{ij}, F_{ij}(k_1)$

R_{ij} is one of the most important turbulence statistic used in the wind energy industry, due to the use of $\langle u'^2 \rangle$ in the definition of turbulence intensity (IEC, 2005b). Unfortunately, it is also one of the most challenging statistic to be obtained from the lidar data, partly due to challenges in data processing, and partly due to economic reasons. If economics is not a major constraint, then three lidars with beams intersecting at one point will provide spatially filtered turbulence statistics (Mann et al., 2009). With two lidars we are restricted to estimating the turbulence statistics of only two components, i.e. horizontal and vertical (Davies et al., 2005; Collier et al., 2005).

Normally, economics of a project is important and we are then restricted to using only one lidar. In this case, a lidar beam can be oriented in the direction of the turbulence statistic that we are interested in estimating. For example, if we are interested in estimating $\langle u'^2 \rangle$, then ideally the lidar beam should be pointed horizontally in the mean wind direction at the height of interest, and for the period within which $\langle u'^2 \rangle$ is obtained (Lawrence et al., 1972). For a ground-based lidar system this would be impossible since the beam would only measure wind that is very close to the ground. Alternatively, we could point the lidar beam at a very small elevation angle and assume that the contributions from the vertical velocity are negligible (Drobinski et al., 2004; Collier et al., 2005; Banta et al., 2006; Pichugina et al., 2008). An open question then is, how small the elevation should be so that the vertical velocity contributions can be neglected? Drobinski et al. (2004), Banta et al. (2006) and Pichugina et al. (2008) neglected the vertical velocity contributions up to an elevation angle of 20° , but provided no justification to the assumption of negligible vertical velocity contributions. This method also requires that the horizontal homogeneity assumption is valid over a larger area, particularly if we are interested to measure turbulence statistics at greater heights and/or several heights. Measurements of $\langle w'^2 \rangle$ can be relatively easier since we need to point the beam only in the vertical direction (Cohn et al., 1998; Tucker et al., 2009).

Lidar turbulence measurements review

A. Sathe and J. Mann

Title Page

Abstract

Introduction

Conclusions

References

Tables

Figures

◀

▶

◀

▶

Back

Close

Full Screen / Esc

Printer-friendly Version

Interactive Discussion



In principle, following Frehlich (1997) and Banakh and Smalikho (1997b) approach, we can then obtain unfiltered $\langle w'^2 \rangle$ from $\langle v_r'^2 \rangle$.

R_{ij} can also be obtained using scanning lidar data, either using the RHI scanning (Gal-Chen et al., 1992; Davies et al., 2003; Davis et al., 2008) or VAD scanning (Eberhard et al., 1989; Mann et al., 2010). If say for a VAD scanning, we use high frequency v_r measurements, deduce the u , v , and w components at every measurement time step, and obtain say $\langle u'^2 \rangle$ or $F_{11}(k_1)$, then apart from the probe volume averaging effect, large systematic errors will also be introduced in the measurement of $\langle u'^2 \rangle$ due to the contamination by the diagonal and cross components of \mathbf{R} (Sathe et al., 2011b; Sathe and Mann, 2012). In such cases, one should be very careful in using the R_{ij} measurements obtained from a scanning lidar, since removing only the probe volume filtering effect (Wagner et al., 2009) without giving consideration to cross-contamination, or neglecting the effects of systematic errors completely (Lang and McKeogh, 2011) will provide erroneous values. Using $\langle v_r'^2 \rangle$ instead of high frequency v_r measurements to obtain R_{ij} is then essential in order to avoid contamination by the components of \mathbf{R} (Eberhard et al., 1989; Gal-Chen et al., 1992; Mann et al., 2010; Sathe, 2012). The unfiltered $\langle v_r'^2 \rangle$ can be obtained using methods suggested by Frehlich (1997) and Mann et al. (2010), and hence obtain unfiltered R_{ij} .

Estimating $F_{ij}(k_1)$ from lidar data is even more challenging than estimating R_{ij} , since we need high frequency measurements of v_r . For a scanning lidar (say VAD), combining high frequency measurements from the lidar beams oriented in different directions result in erroneous measurements of $F_{ij}(k_1)$ (Canadillas et al., 2010; Sathe and Mann, 2012). Most studies in the past have thus used either a staring lidar configuration (Lawrence et al., 1972; Davies et al., 2005; Lothon et al., 2009; O'Connor et al., 2010), or neglected contributions from the w component at small elevation angles (Hardesty et al., 1982; Drobinski et al., 2004).

Lidar turbulence measurements review

A. Sathe and J. Mann

Title Page

Abstract

Introduction

Conclusions

References

Tables

Figures



Back

Close

Full Screen / Esc

Printer-friendly Version

Interactive Discussion



4.2.4 $\langle w'^3 \rangle$, $\langle w'\theta' \rangle$, $\text{coh}_{ij}(k_1)$

Very little efforts have been focused on the estimation of $\langle w'^3 \rangle$, $\langle w'\theta' \rangle$ and $\text{coh}_{ij}(k_1)$. One of the reasons could be the complexity of data processing and the associated errors that present great challenges in their estimations. Particularly, in the estimation of $\langle w'\theta' \rangle$, apart from estimating ε , it also requires estimation of either $\langle w'^3 \rangle$ (Gal-Chen et al., 1992), or $\langle w'^2 \rangle$ (Davis et al., 2008). Estimating higher order moments, particularly third and fourth order, introduce large errors in the measurements (Lenschow et al., 1994, 2000). Fortunately, we can reduce the errors in higher moments using the autocorrelation technique (Lenschow et al., 2000) or the spectral technique (Frehlich et al., 1998), which increase the potential of estimating the heat flux using Eq. (35).

5 Turbulence quantities of interest for future applications in wind energy

Wind turbines have been and will be installed in different parts of the world, where the atmospheric conditions differ significantly from each other. The motivation for why turbulence is important for wind energy purposes is already given in Sect. 1. Here we will specifically discuss those parameters listed in Table 1 that are useful for wind energy. According to IEC (2005a) standards, a wind turbine should be designed for different classes of turbulence intensities. The turbulence intensity I is defined as the ratio of standard deviation of the u component to the mean horizontal wind speed ($I = \sqrt{\langle u'^2 \rangle} / \langle u \rangle$). It is thus crucial to perform measurements of $\langle u'^2 \rangle$. Apart from I , it also important to measure the mean wind speed profile, which is dependent on the velocity covariances $\langle u'w' \rangle$ and $\langle v'w' \rangle$ (Wyngaard, 2010). The diagonal components of \mathbf{R} , i.e. $\langle u'^2 \rangle$, $\langle v'^2 \rangle$ and $\langle w'^2 \rangle$ influence the loads significantly. Thus for wind energy purposes, it is very important to measure R_{ij} , but to do it using lidars, from Eq. (12) we see that we need measurements of $\langle v_r'^2 \rangle$. In order to get unfiltered $\langle v_r'^2 \rangle$ measurements, as seen in

Title Page

Abstract

Introduction

Conclusions

References

Tables

Figures

◀

▶

◀

▶

Back

Close

Full Screen / Esc

Printer-friendly Version

Interactive Discussion



Sect. 4, with the current state-of-the-art methods, we need to fit lidar measurements of $\tilde{D}(r)$ and/or $\tilde{F}(k_1)$ to some isotropic or anisotropic turbulence models.

A current practice in the wind energy industry to perform load simulations is that a turbulent wind field is generated using either the Mann (1994) model or an empirical Kaimal et al. (1972) spectrum is combined with some coherence model (IEC, 2005a). As discussed in Sect. 2, the need to measure ε and \mathcal{L} is then clearly evident. These parameters are normally obtained by fitting the Mann (1994) model to the measurements of $F_{ij}(k_1)$, which could be obtained using lidars. \mathcal{L} and coh_{ij} are important for estimating the loads and wake meandering (Larsen et al., 2008). The influence of atmospheric stability on wind speed profile and on wind turbine loads is becoming increasingly evident (Sathe et al., 2011a, 2012). To this extent, measurement of $\langle w'\theta' \rangle$ is quite important for wind energy. According to Lenschow et al. (1994), ℓ_{ij} is useful in estimating the averaging time required to keep the random errors below a certain threshold for a particular turbulence statistic, and hence is a desirable measurement quantity for wind energy purposes.

Recently lidars are being contemplated to be used for wind turbine control. The concept is such that either the lidar is placed on a nacelle of a wind turbine (Schlipf et al., 2012), or mounted inside a spinner (Mikkelsen et al., 2012; Simley et al., 2013) to detect the incoming wind field, and carry out a feed-forward control to reduce the structural loads on a wind turbine. The degree to which such a concept can be applied successfully depends on how well the lidars are able to detect the incoming turbulent structures. From Sathe et al. (2012) we understand that different components of a wind turbine are affected by different scales of turbulent structures. It is thus important to be able to detect range of turbulence scales, up to the order of or less than the probe volume length.

Lidar turbulence measurements review

A. Sathe and J. Mann

Title Page

Abstract

Introduction

Conclusions

References

Tables

Figures

◀

▶

◀

▶

Back

Close

Full Screen / Esc

Printer-friendly Version

Interactive Discussion



6 Summary and Discussion

Figure 4 summarizes the number of studies that have significantly contributed in the research on turbulence measurements using wind lidars from 1972–2012. Research with lidar turbulence measurements dates back to 1972, but it was not until 1997 that the publication rate picked up pace. If we consider that the lidar turbulence measurement research encompasses the period between 1972–2012, then more than 80 % of the research was carried out in the latter half of the 30 yr period, i.e. from 1997–2012. In the first 15 yr of development, barring the works of Smalikho (1995) and Banakh et al. (1996), focus was more on extracting turbulence information without taking into account probe volume averaging (see Sect. 4). Since then substantial effort has been put into modelling the averaging effect inside the lidar probe volume, mainly by Professor V. A. Banakh and Dr. I. N. Smalikho from the V. E. Zuev Institute of Atmospheric Optics of Russian Academy of Sciences, Siberian Branch, Russia, and the late Dr. R. Frehlich from the University of Colorado, USA. Interestingly, they pioneered new processing algorithms independently of each other roughly during the same period, i.e. from the mid 1990s until the mid 2000s, wherein they demonstrated how to extract unfiltered turbulence parameters (Smalikho, 1995; Banakh et al., 1996; Frehlich, 1997; Banakh and Smalikho, 1997b; Smalikho et al., 2005; Frehlich et al., 2006). We believe that this development has significantly contributed to the number of research studies carried out in the last 15 yr. Further development in processing algorithms will also greatly benefit from their works. We expect that the number of such studies will continue to increase due to increase in wind energy development all over the world.

That brings us to an obvious question; *is there anything new to be discovered with regards to processing raw lidar data, scanning configurations, or the technology itself that can provide more reliable turbulence measurements using lidars?* We attempt to answer this question as follows:

1. Raw lidar data processing – up until now, the processing algorithms that have been developed have shown that by combining an isotropic turbulence model

AMTD

6, 6815–6871, 2013

Lidar turbulence measurements review

A. Sathe and J. Mann

Title Page

Abstract

Introduction

Conclusions

References

Tables

Figures



Back

Close

Full Screen / Esc

Printer-friendly Version

Interactive Discussion



Lidar turbulence measurements review

A. Sathe and J. Mann

Title Page

Abstract

Introduction

Conclusions

References

Tables

Figures

◀

▶

◀

▶

Back

Close

Full Screen / Esc

Printer-friendly Version

Interactive Discussion

with lidar measurements, we are able to estimate ε , $\langle v_r'^2 \rangle$ and \mathcal{L} (see Table 1). However, turbulence is not isotropic in all range of scales. Anisotropy is particularly observed on bigger length scales, and thus it is more desirable to estimate $\langle v_r'^2 \rangle$, \mathcal{L} by combining an anisotropic turbulence model (Kristensen et al., 1989; Mann, 1994) with the lidar measurements. This recommendation was also made by Frehlich et al. (2006) and Frehlich and Kelley (2008). There is however a need for developing algorithms that make as little use of models as possible in combination with the measurements. Even an anisotropic turbulence model such as Mann (1994) is based on a set of assumptions, e.g. neutral atmospheric conditions, applicability in the surface layer, validity of Taylor's hypothesis, and it does not apply to complex terrain. If we then combine such a model with lidar measurements, and estimate turbulence parameters then additional uncertainties may be introduced. In order to avoid such situations, further developments of algorithms should also focus on making use of only the raw lidar data to extract turbulence parameters, e.g. as shown in Mann et al. (2010). Furthermore, from the study by Sathe et al. (2011b) and Sathe and Mann (2012) it is now clear that in a VAD scanning configuration, obtaining u , v and w components from v_r data at each time step and then deducing turbulence statistics will introduce large systematic errors in the turbulence measurements. One might argue that under some conditions the lidar to sonic correlation may be close to one, but as shown in Sathe et al. (2011b), the correlation would depend on the type of lidar (c-w or pulsed), and the turbulence structure. The correlations with any reference instrument may not be repeatable if the experiment is conducted during different times of the day. It is thus recommended that such data processing method should not be followed. Alternatively, as shown by Wilson (1970), Kropfli (1986), Eberhard et al. (1989) and Mann et al. (2010), using $\langle v_r'^2 \rangle$ instead of v_r to deduce R_{ij} is a fundamentally correct method to extract turbulence information from the raw lidar data.

Lidar turbulence measurements review

A. Sathe and J. Mann

Title Page

Abstract

Introduction

Conclusions

References

Tables

Figures

◀

▶

◀

▶

Back

Close

Full Screen / Esc

Printer-friendly Version

Interactive Discussion

2. Scanning configurations – three measurement configurations have been used until now; staring, VAD, and RHI scanning (see Sect. 3 for details of the scanning configurations). Ideally, using three staring lidars with their beams crossing at a point (similar to sonic anemometer) would provide more reliable measurements as compared to using a single lidar in a VAD or RHI scanning mode. A step in this direction is the use of two lidars (Davies et al., 2004, 2005; Collier et al., 2005). In the VAD or RHI scanning, the assumption of horizontal homogeneity is inevitable, and thus restrict their applicability for wind energy purposes, particularly in complex terrain. Bingöl et al. (2009) provided a technique to correct for terrain induced inhomogeneities in the mean flow. For turbulence measurements we can use Taylor series expansion in the horizontal plane as shown by Frisch (1991). However, the reliability of this algorithm has not been investigated thoroughly, but is a potential study for the future. On the other hand, using three lidars can increase the cost of a project significantly, and hence hinder their use for wind energy development. If we use a single staring lidar at one height then it becomes almost inevitable to combine a turbulence model with lidar measurements in order to extract turbulence information (Smalikho, 1995). Another aspect to be considered when deciding on the scanning configuration is the sampling frequency. Again in this regard the staring configuration will provide faster measurements than the scanning configurations. In a VAD scanning there is a scope for reducing the number of measurement points on a scanning circle. As shown by Eq. (12) we need only six beams at different azimuth and half-opening angles to estimate R_{ij} . However, using random six points will introduce random errors in the turbulence measurements. Sathe (2012) provided some initial calculations of the optimum configuration that would minimize the random errors. The sampling frequency will thus be increased, but further investigations are required.
3. Improvement in lidar technology – new cheaper solid state lasers for coherent detection lidars with integrated optical amplification are being developed and tested (Hansen and Pedersen, 2008; Rodrigo and Pedersen, 2008). These may

Lidar turbulence measurements review

A. Sathe and J. Mann

Title Page

Abstract

Introduction

Conclusions

References

Tables

Figures

◀

▶

◀

▶

Back

Close

Full Screen / Esc

Printer-friendly Version

Interactive Discussion



greatly expand the use of lidars for wind measurements, but they are not specifically tailored for turbulence measurements. Preliminary tests of these lidars have been carried out in Rodrigo and Pedersen (2012) showing good comparison with a sonic anemometer. The solid state lasers with integrated amplification may in the near future compete with the more expensive lasers used in c-w Doppler lidars. Direct detection is still on an experimental level (McKay, 1998) and has only been used in the atmosphere sporadically (Xia et al., 2007; Dors et al., 2011). The simple design of these instrument may eventually lead to cheaper lidars systems. Non-coherent detection may also provide possible new ways to estimate atmospheric turbulence (Mayor et al., 2012; Sela and Tsadka, 2011), but to our knowledge they do not, so far, challenge capabilities of the coherent Doppler lidars.

In order to meet the objectives stated above, a simulation study can significantly help in planning and designing the experiments better (Frehlich and Cornman, 2002; Banakh and Werner, 2005). A perhaps important aspect of turbulence measurements using lidars that we have not considered in this review is the instrumental error, which is generally assumed to be uncorrelated (Frehlich et al., 1998; Lenschow et al., 2000). Fortunately, for modern commercial lidar systems, the magnitude of the instrumental error is not significant, and can be safely neglected (Mann et al., 2009). However, for those lidar instruments, which have significant instrumental error, and can potentially bias turbulence measurements, the techniques suggested by Frehlich et al. (1998), Drobinski et al. (2000) and Lenschow et al. (2000) can be used to correct for them.

Acknowledgements. This work is carried out as a part of a research project funded by the Danish Ministry of Science, Innovation and Higher Education – Technology and Production, grant no. 11-117018. The resources provided by the Center for Computational Wind Turbine Aerodynamics and Atmospheric Turbulence funded by the Danish Council for Strategic Research grant no. 09-067216 are also acknowledged. We also thank Erik Juul from DTU Wind Energy department for helping with the sketches of the scanning configurations.

References

- Abramowitz, M. and Stegun, I. A. (Eds.): Handbook of Mathematical Functions, 9th Edn., Dover Publications, INC., New York, 1965. 6840
- Angelou, N., Mann, J., Sjöholm, M., and Courtney, M.: Direct measurement of the spectral transfer function of a laser based anemometer, Rev. Sci. Instrum., 83, 033111, doi:10.1063/1.3697728, 2012. 6865
- Banakh, V. A. and Smalikho, I. N.: Determination of the turbulent energy dissipation rate from lidar sensing data, Atmos. Ocean. Optics, 10, 295–302, 1997a. 6843, 6844, 6864
- Banakh, V. A. and Smalikho, I. N.: Estimation of the turbulence energy dissipation rate from the pulsed Doppler lidar data, Atmos. Ocean. Optics, 10, 957–965, 1997b. 6839, 6840, 6844, 6847, 6850, 6864, 6865
- Banakh, V. A. and Werner, C.: Computer simulation of coherent Doppler lidar measurement of wind velocity and retrieval of turbulent wind statistics, Opt. Eng., 44, 071205, doi:10.1117/1.1955167, 2005. 6818, 6844, 6845, 6853, 6864
- Banakh, V. A., Smalikho, I. N., Köpp, F., and Werner, C.: Representativeness of wind measurements with a CW Doppler lidar in the atmospheric boundary layer, Appl. Optics, 34, 2055–2067, doi:10.1364/AO.34.002055, 1995. 6843
- Banakh, V. A., Werner, C., Kerkis, N. N., Köpp, F., and Smalikho, I. N.: Turbulence measurements with a CW Doppler lidar in the atmospheric boundary layer, Atmos. Ocean. Optics, 8, 955–959, 1995b. 6843, 6864
- Banakh, V. A., Werner, C., Köpp, F., and Smalikho, I. N.: Measurement of turbulent energy dissipation rate with a scanning Doppler lidar, Atmos. Ocean. Optics, 9, 849–853, 1996. 6835, 6837, 6838, 6843, 6844, 6845, 6850, 6864
- Banakh, V. A., Werner, C., Köpp, F., and Smalikho, I. N.: Fluctuation spectra of wind velocity measured with a Doppler lidar, Atmos. Ocean. Optics, 10, 202–208, 1997. 6843, 6864, 6865
- Banakh, V. A., Smalikho, I. N., Köpp, F., and Werner, C.: Measurements of turbulent energy dissipation rate with a CW Doppler lidar in the atmospheric boundary layer, J. Atmos. Ocean. Tech., 16, 1044–1061, doi:10.1175/1520-0426(1999)016<1044:MOTEDR>2.0.CO;2, 1999. 6834, 6844, 6845, 6864, 6865
- Banakh, V. A., Smalikho, I. N., Pichugina, Y. L., and Brewer, W. A.: Representativeness of measurements of the dissipation rate of turbulence energy by scanning Doppler lidar, Atmos. Ocean Optics, 23, 48–54, doi:10.1134/S1024856010010100, 2010. 6844, 6864, 6865

Lidar turbulence measurements review

A. Sathe and J. Mann

Title Page

Abstract

Introduction

Conclusions

References

Tables

Figures

◀

▶

◀

▶

Back

Close

Full Screen / Esc

Printer-friendly Version

Interactive Discussion



Lidar turbulence measurements review

A. Sathe and J. Mann

Title Page

Abstract

Introduction

Conclusions

References

Tables

Figures

◀

▶

◀

▶

Back

Close

Full Screen / Esc

Printer-friendly Version

Interactive Discussion



- Banta, R. M., Pichugina, Y. L., and Brewer, W. A.: Turbulent velocity-variance profiles in the stable boundary layer generated by a nocturnal low-level jet, *J. Atmos. Sci.*, 63, 2700–2719, doi:10.1175/JAS3776.1, 2006. 6846, 6864
- Bingöl, F., Mann, J., and Foussekis, D.: Conically scanning lidar error in complex terrain, *Meteorol. Z.*, 18, 189–195, doi:10.1127/0941-2948/2009/0368, 2009. 6852
- Branlard, E., Pedersen, A. T., Mann, J., Angelou, N., Fischer, A., Mikkelsen, T., Harris, M., Slinger, C., and Montes, B. F.: Retrieving wind statistics from average spectrum of continuous-wave lidar, *Atmos. Meas. Tech.*, 6, 1673–1683, doi:10.5194/amt-6-1673-2013, 2013. 6845, 6864
- Browning, K. A. and Wexler, R.: The determination of kinematic properties of a wind field using a Doppler radar, *J. Appl. Meteorol.*, 7, 105–113, doi:10.1175/1520-0450(1968)007<0105:TDOKPO>2.0.CO;2, 1968. 6824
- Burton, T., Sharpe, D., Jenkins, N., and Bossanyi, E.: *Wind Energy Handbook*, John Wiley and Sons, LTD, 2001. 6817
- Canadillas, B., Bégué, A., and Neumann, T.: Comparison of turbulence spectra derived from LiDAR and sonic measurements at the offshore platform FINO1, in: *DEWEK 2010, 10th German Wind Energy Conference*, Bremen, Germany, 2010. 6847, 6865
- Chan, P. W.: Generation of an eddy dissipation rate map at the Hong Kong international airport based on Doppler lidar data, *J. Atmos. Ocean. Tech.*, 28, 37–49, doi:10.1175/2010JTECHA1458.1, 2011. 6844, 6864, 6865
- Cohn, S. A., Mayor, S. D., Grund, C. J., Weckwerth, T. M., and Senff, C.: The lidars in flat terrain (LIFT) experiment, *B. Am. Meteorol. Soc.*, 79, 1329–1343, doi:10.1175/1520-0477(1998)079<1329:TLIFTL>2.0.CO;2, 1998. 6844, 6846, 6864, 6865
- Collier, C. G., Davies, F., Bozier, K. E., Holt, A. R., Middleton, D. R., Pearson, G. N., Siemen, S., Willetts, D. V., Upton, G. J. G., and Young, R. I.: Dual-Doppler lidar measurements for improving dispersion models, *B. Am. Meteorol. Soc.*, 86, 825–838, doi:10.1175/BAMS-86-6-825, 2005. 6843, 6844, 6846, 6852, 6864
- Davies, F., Collier, C. G., Bozier, K. E., and Pearson, G. N.: On the accuracy of retrieved wind information from Doppler lidar observation, *Q. J. Roy. Meteorol. Soc.*, 129, 321–334, doi:10.1256/qj.01.126, 2003. 6847, 6864
- Davies, F., Collier, C. G., Pearson, G. N., and Bozier, K. E.: Doppler lidar measurements of turbulent structure function over an urban area, *J. Atmos. Ocean. Tech.*, 21, 753–

Lidar turbulence measurements review

A. Sathe and J. Mann

Title Page

Abstract

Introduction

Conclusions

References

Tables

Figures



Back

Close

Full Screen / Esc

Printer-friendly Version

Interactive Discussion

761, doi:10.1175/1520-0426(2004)021<0753:DLMOTS>2.0.CO;2, 2004. 6844, 6845, 6852, 6864, 6865

Davies, F., Collier, C. G., and Bozier, K. E.: Errors associated with dual-Doppler-lidar turbulence measurements, *J. Opt. A-Pure Appl. Op.*, 7, S280–S289, doi:10.1088/1464-4258/7/6/005, 2005. 6843, 6844, 6846, 6847, 6852, 6864, 6865

Davis, J. C., Collier, C. G., Davies, F., and Bozier, K. E.: Spatial variations of sensible heat flux over an urban area measured using Doppler lidar, *Meteorol. Appl.*, 15, 367–380, doi:10.1002/met.79, 2008. 6843, 6847, 6848, 6864, 6865

Dors, I., McHugh, J. P., Jumper, G. Y., and Roadcap, J.: Velocity spectra and turbulence using direct detection lidar and comparison with thermosonde measurements, *J. Geophys. Res.*, 116, D01102, doi:10.1029/2010JD014606, 2011. 6843, 6853, 6864, 6865

Drobinski, P., Brown, R. A., Flamant, P. H., and Pelon, J.: Evidence of organized large eddies by ground-based Doppler lidar, sonic anemometer and sodar, *Bound.-Lay. Meteorol.*, 88, 343–361, doi:10.1023/A:1001167212584, 998. 6865

Drobinski, P., Dabas, A. M., and Flamant, P. H.: Remote measurement of turbulent wind spectra by heterodyne Doppler lidar technique, *J. Appl. Meteorol.*, 39, 2434–2451, doi:10.1175/1520-0450(2000)039<2434:RMOTWS>2.0.CO;2, 2000. 6835, 6843, 6844, 6853, 6864, 6865

Drobinski, P., Carlotti, P., Newsom, R. K., Banta, R. M., Foster, R. C., and Redelsperger, J.-L.: The structure of the near-neutral atmospheric surface layer, *J. Atmos. Sci.*, 61, 699–714, doi:10.1175/1520-0469(2004)061<0699:TSOTNA>2.0.CO;2, 2004. 6846, 6847, 6864, 6865

Eberhard, W. L., Cupp, R. E., and Healy, K. R.: Doppler lidar measurements of profiles of turbulence and momentum flux, *J. Atmos. Ocean. Tech.*, 6, 809–819, doi:10.1175/1520-0426(1989)006<0809:DLMOPO>2.0.CO;2, 1989. 6827, 6828, 6845, 6847, 6851, 6864

Emeis, S., Harris, M., and Banta, R. M.: Boundary-layer anemometry by optical remote sensing for wind energy applications, *Meteorol. Z.*, 16, 337–347, doi:10.1127/0941-2948/2007/0225, 2007. 6817

Engelbart, D. A. M., Kallistratova, M., and Kouznetsov, R.: Determination of the turbulent fluxes of heat and momentum in the ABL by ground-based remote-sensing techniques (a review), *Meteorol. Z.*, 16, 325–335, doi:10.1127/0941-2948/2007/0224, 2007. 6817

Frehlich, R.: Coherent Doppler lidar signal covariance including wind shear and wind turbulence, *Appl. Optics*, 33, 6472–6481, doi:10.1364/AO.33.006472, 1994. 6818, 6833



Lidar turbulence measurements review

A. Sathe and J. Mann

Title Page

Abstract

Introduction

Conclusions

References

Tables

Figures

◀

▶

◀

▶

Back

Close

Full Screen / Esc

Printer-friendly Version

Interactive Discussion



- Frehlich, R.: Effects of wind turbulence on coherent Doppler lidar performance, *J. Atmos. Ocean. Tech.*, 14, 54–75, doi:10.1175/1520-0426(1997)014<0054:EOWTOC>2.0.CO;2, 1997. 6838, 6839, 6840, 6843, 6844, 6845, 6847, 6850, 6864, 6865
- 5 Frehlich, R. and Cornman, L.: Estimating spatial velocity statistics with coherent Doppler lidar, *J. Atmos. Ocean. Tech.*, 19, 355–366, doi:10.1175/1520-0426-19.3.355, 2002. 6844, 6845, 6853, 6864, 6865
- Frehlich, R. and Kelley, N.: Measurements of wind and turbulence profiles with scanning Doppler lidar for wind energy applications, *IEEE J. Sel. Top. Appl.*, 1, 42–47, doi:10.1109/JSTARS.2008.2001758, 2008. 6841, 6844, 6845, 6851, 6864
- 10 Frehlich, R., Hannon, S. M., and Henderson, S. W.: Performance of a 2- μm coherent Doppler lidar for wind measurements, *J. Atmos. Ocean. Tech.*, 11, 1517–1528, doi:10.1175/1520-0426(1994)011<1517:POACDL>2.0.CO;2, 1994. 6833, 6844, 6864, 6865
- Frehlich, R., Hannon, S. M., and Henderson, S. W.: Coherent Doppler lidar measurements of wind field statistics, *Bound.-Lay. Meteorol.*, 86, 233–256, doi:10.1023/A:1000676021745, 15 1998. 6835, 6841, 6844, 6845, 6848, 6853, 6864, 6865
- Frehlich, R., Meillier, Y., Jensen, M. L., Balsley, B., and Sharman, R.: Measurements of boundary layer profiles in urban environment, *J. Appl. Meteorol. Clim.*, 45, 821–837, doi:10.1175/JAM2368.1, 2006. 6841, 6844, 6845, 6850, 6851, 6864
- Frehlich, R., Meillier, Y., and Jensen, M. L.: Measurements of boundary layer profiles with in situ sensors and Doppler lidar, *J. Atmos. Ocean. Tech.*, 25, 1328–1340, 20 2008. 6844, 6864, 6865
- Frisch, A. S.: On the measurement of second moments of turbulent wind velocity with a single Doppler radar over non-homogeneous terrain, *Bound.-Lay. Meteorol.*, 54, 29–39, doi:10.1007/BF00119410, 1991. 6828, 6852
- 25 Gal-Chen, T., Xu, M., and Eberhard, W. L.: Estimation of atmospheric boundary layer fluxes and other turbulence parameters from Doppler lidar data, *J. Geophys. Res.*, 97, 18409–18423, doi:10.1029/91JD03174, 1992. 6831, 6843, 6845, 6847, 6848, 6864, 6865
- Gottschall, J. and Peinke, J.: How to improve the estimation of power curves for wind turbines, *Environ. Res. Lett.*, 3, 015005, doi:10.1088/1748-9326/3/1/015005, 2008. 6817
- 30 Hansen, R. S. and Pedersen, C.: All semiconductor laser doppler anemometer at 1.55 μm , *Opt. Express*, 16, 18288–18295, doi:10.1364/OE.16.018288, 2008. 6852

Lidar turbulence measurements review

A. Sathe and J. Mann

Title Page

Abstract

Introduction

Conclusions

References

Tables

Figures

◀

▶

◀

▶

Back

Close

Full Screen / Esc

Printer-friendly Version

Interactive Discussion



Hardesty, R. M. and Darby, L. S.: Ground-based and airborne lidar, in: *Encyclopedia of Hydrological Sciences*, edited by: Anderson, M. G., John Wiley & Sons, Ltd., doi:10.1002/0470848944.hsa052, 2005. 6818

Hardesty, R. M., Korrell, J. A., and Hall, F. F.: Lidar measurement of wind velocity turbulence spectra encountered by a rotating turbine blade, Tech. Rep. DOE/RL/10236–81/1, National Oceanic and Atmospheric Administration, Boulder, CO, USA, 1982. 6827, 6847, 6865

IEC: IEC 61400–1, Wind turbines – Part 1: Design Requirements, International Electrotechnical Commission, Geneva, Switzerland, 2005a. 6817, 6848, 6849

IEC: IEC 61400–3, Offshore wind turbines – Part 1: Design Requirements, International Electrotechnical Commission, Geneva, Switzerland, 2005b. 6846

Kaimal, J. C. and Finnigan, J. J.: Acquisition and processing of atmospheric boundary layer data, in: *Atmospheric Boundary Layer Flows*, no. 7, Oxford University Press, NY, 255–257, 1994. 6824

Kaimal, J. C., Wyngaard, J. C., Izumi, Y., and Coté, O. R.: Spectral characteristics of surface-layer turbulence, *Q. J. Roy. Meteorol. Soc.*, 98, 563–589, doi:10.1002/qj.49709841707, 1972. 6839, 6841, 6845, 6849

Kaiser, K., Langreder, W., Hohlen, H., and Højstrup, J.: Turbulence correction for power curves, in: *Wind Energy, Proceedings of the Euromech Colloquium*, edited by: Peinke, J., Schumann, P., and Barth, S., Springer, 159–162, 2007. 6817

Kindler, D., Oldroyd, A., Macaskill, A., and Finch, D.: An eight month test campaign of the QinetiQ ZephIR system: preliminary results, *Meteorol. Z.*, 16, 479–489, doi:10.1127/0941-2948/2007/0226, 2007. 6817

Kristensen, L., Lenschow, D. H., Kirkegaard, P., and Courtney, M.: The spectral velocity tensor for homogeneous boundary-layer turbulence, *Bound.-Lay. Meteorol.*, 47, 149–193, doi:10.1007/BF00122327, 1989. 6837, 6851

Kristensen, L., Kirkegaard, P., Mann, J., Mikkelsen, T., Nielsen, M., and Sjöholm, M.: Determining the velocity fine structure by a laser anemometer with fixed orientation, Tech. Rep. Risø-R-1744(EN), Risø DTU, 2010. 6865

Kristensen, L., Kirkegaard, P., and Mikkelsen, T.: Determining the velocity fine structure by a laser anemometer with fixed orientation, Tech. Rep. Risø-R-1762(EN), Risø DTU, 2011. 6834, 6835, 6837, 6839, 6840, 6843, 6864, 6865

Lidar turbulence measurements review

A. Sathe and J. Mann

Title Page

Abstract

Introduction

Conclusions

References

Tables

Figures

◀

▶

◀

▶

Back

Close

Full Screen / Esc

Printer-friendly Version

Interactive Discussion



- Kristensen, L., Kirkegaard, P., and Mikkelsen, T.: Determining the velocity fine structure by a laser anemometer in VAD operation, Tech. Rep. DTU Wind Energy E-0008(EN), DTU Wind Energy, Lyngby, Denmark, 2012. 6835, 6836, 6837, 6844, 6845, 6864, 6865
- 5 Kropfli, R. A.: Single Doppler radar measurement of turbulence profiles in the convective boundary layer, *J. Atmos. Ocean. Tech.*, 3, 305–314, doi:10.1175/1520-0426(1986)003<0305:SDRMOT>2.0.CO;2, 1986. 6826, 6851
- Kunkel, K. E., Eloranta, E. W., and Weinman, J. A.: Remote determination of winds, turbulence spectra and energy dissipation rates in the boundary layer from lidar measurements, *J. Atmos. Sci.*, 37, 978–985, doi:10.1175/1520-0469(1980)037<0978:RDOWTS>2.0.CO;2, 1980. 6826, 6864
- 10 Lang, S. and McKeogh, E.: Lidar and sodar measurements of wind speed and direction in upland terrain for wind energy purposes, *Remote Sens.*, 3, 1871–1901, doi:10.3390/rs3091871, 2011. 6847, 6864
- Larsen, G. C., Madsen, H. A., Thomsen, K., and Larsen, T. J.: Wake meandering: a pragmatic approach, *Wind Energy*, 11, 377–395, doi:10.1002/we.267, 2008. 6849
- 15 Lawrence, T. R., Wilson, D. J., Craven, C. E., Jones, I. P., Huffaker, R. M., and Thomson, J. A. L.: A laser velocimeter for remote wind sensing, *Rev. Sci. Instrum.*, 43, 512–518, doi:10.1063/1.1685674, 1972. 6826, 6846, 6847, 6865
- Lenschow, D. H., Mann, J., and Kristensen, L.: How long is long enough when measuring fluxes and other turbulence statistics?, *J. Atmos. Ocean. Tech.*, 11, 661–673, 1994. 6833, 6848, 6849
- 20 Lenschow, D. H., Wulfmeyer, V., and Senff, C.: Measuring second- through fourth-order moments in noisy data, *J. Atmos. Ocean. Tech.*, 17, 1330–1347, doi:10.1175/1520-0426(2000)017<1330:MSTFOM>2.0.CO;2, 2000. 6848, 6853, 6865
- 25 Lhermitte, R. M.: Note on wind variability with Doppler radar, *J. Atmos. Sci.*, 19, 343–346, doi:10.1175/1520-0469(1962)019<0343:NOWVWD>2.0.CO;2, 1962. 6824
- Lhermitte, R. M.: Note on the observation of small-scale atmospheric turbulence by Doppler radar techniques, *Radio Sci.*, 4, 1241–1246, doi:10.1029/RS004i012p01241, 1969. 6825
- 30 Lothon, M., Lenschow, D. H., and Mayor, S. D.: Coherence and scale of vertical velocity in the convective boundary layer from a Doppler lidar, *Bound.-Lay. Meteorol.*, 121, 521–536, doi:10.1007/s10546-006-9077-1, 2006. 6844, 6864, 6865

Lidar turbulence measurements review

A. Sathe and J. Mann

Title Page

Abstract

Introduction

Conclusions

References

Tables

Figures

◀

▶

◀

▶

Back

Close

Full Screen / Esc

Printer-friendly Version

Interactive Discussion



- Lothon, M., Lenschow, D. H., and Mayor, S. D.: Doppler lidar measurements of vertical velocity spectra in the convective planetary boundary layer, *Bound.-Lay. Meteorol.*, 132, 205–226, doi:10.1007/s10546-009-9398-y, 2009. 6843, 6844, 6847, 6864, 6865
- 5 Mann, J.: The spatial structure of neutral atmospheric surface-layer turbulence, *J. Fluid Mech.*, 273, 141–168, doi:10.1017/S0022112094001886, 1994. 6821, 6841, 6845, 6849, 6851
- Mann, J., Cariou, J., Courtney, M., Parmentier, R., Mikkelsen, T., Wagner, R., Lindelow, P., Sjöholm, M., and Enevoldsen, K.: Comparison of 3D turbulence measurements using three staring wind lidars and a sonic anemometer, *Meteorol. Z.*, 18, 135–140, doi:10.1127/0941-2948/2009/0370, 2009. 6835, 6843, 6846, 6853, 6865
- 10 Mann, J., Peña, A., Bingöl, F., Wagner, R., and Courtney, M. S.: Lidar scanning of momentum flux in and above the surface layer, *J. Atmos. Ocean. Tech.*, 27, 792–806, doi:10.1175/2010JTECHA1389.1, 2010. 6834, 6841, 6842, 6845, 6847, 6851, 6864
- Mayor, S. D., Lenschow, D. H., Schwiesow, R. L., Mann, J., Frush, C. L., and Simon, M. K.: Validation of NCAR 10.6- μm CO₂ Doppler lidar radial velocity measurements and comparison with a 915-MHz profiler, *J. Atmos. Ocean. Tech.*, 14, 1110–1126, doi:10.1175/1520-0426(1997)014<1110:VONMCD>2.0.CO;2, 1997. 6864, 6865
- 15 Mayor, S. D., Lowe, J. P., and Mauzey, C. F.: Two-component horizontal aerosol motion vectors in the atmospheric surface layer from a cross-correlation algorithm applied to scanning elastic backscatter lidar data, *J. Atmos. Ocean. Tech.*, 29, 1585–1602, doi:10.1175/JTECHD-11-00225.1, 2012. 6853
- 20 McKay, J. A.: Modeling of direct detection Doppler wind lidar, I. The edge technique, *Appl. Optics*, 37, 6480–6486, doi:10.1364/AO.37.006480, 1998. 6853
- Measures, R. M.: *Laser Remote Sensing: Fundamentals and Applications*, Krieger Publishing Company, Malabar, Florida, 524 pp., 1984. 6821
- 25 Mikkelsen, T., Angelou, N., Hansen, K., Sjöholm, M., Harris, M., Slinger, C., Hadley, P., Scullion, R., Ellis, G., and Vives, G.: A spinner-integrated wind lidar for enhanced wind turbine control, *Wind Energy*, doi:10.1002/we.1564, in press, 2012. 6849
- O'Connor, E. J., Illingworth, A. J., Brooks, I. M., Westbrook, C. D., Hogan, R. J., Davies, F., and Brooks, B. J.: A method for estimating the turbulent kinetic energy dissipation rate from a vertically pointing Doppler lidar, and independent evaluation from balloon-borne in situ measurements, *J. Atmos. Ocean. Tech.*, 27, 1652–1664, doi:10.1175/2010JTECHA1455.1, 2010. 6843, 6847, 6864, 6865
- 30

Lidar turbulence measurements review

A. Sathe and J. Mann

Title Page

Abstract

Introduction

Conclusions

References

Tables

Figures

◀

▶

◀

▶

Back

Close

Full Screen / Esc

Printer-friendly Version

Interactive Discussion



laser anemometers and providing output data that represents wind characteristics, Patent no. WO2011036553-A1, 2011. 6853

Simley, E., Pao, L. Y., Frehlich, R., Jonkman, B., and Kelley, N.: Analysis of light detection and ranging wind speed measurements for wind turbine control, *Wind Energy*, doi:10.1002/we.1584, in press, 2013. 6849

Sjöholm, M., Mikkelsen, T., Mann, J., Enevoldsen, K., and Courtney, M.: Spatial averaging-effects on turbulence measured by a continuous-wave coherent lidar, *Meteorol. Z.*, 18, 281–287, doi:10.1127/0941-2948/2009/0379, 2009. 6843, 6865

Smalikho, I., Kopp, F., and Rahm, S.: Measurement of atmospheric turbulence by 2- μm Doppler lidar, *J. Atmos. Ocean. Tech.*, 22, 1733–1747, doi:10.1175/JTECH1815.1, 2005. 6840, 6843, 6844, 6850, 6864

Smalikho, I. N.: On measurement of dissipation rate of the turbulent energy with a CW Doppler lidar, *Atmos. Ocean. Optics*, 8, 788–793, 1995. 6833, 6834, 6835, 6837, 6838, 6839, 6843, 6850, 6852

Smith, D. A., Harris, M., Coffey, A. S., Mikkelsen, T., Jørgensen, H. E., Mann, J., and Danielian, R.: Wind lidar evaluation at the danish wind test site in Høvsøre, *Wind Energy*, 9, 87–93, doi:10.1002/we.193, 2006. 6817

Sonnenschein, C. M. and Horrigan, F. A.: Signal-to-noise relationships for coaxial systems that heterodyne backscatter from atmosphere, *Appl. Optics*, 10, 1600, doi:10.1364/AO.10.001600, 1971. 6834

Taylor, G. I.: The spectrum of Turbulence, *P. Roy. Soc. Lond. A*, 164, 476–490, 1938. 6835

Tucker, S. C., Brewer, W. A., Banta, R. M., Senff, C. J., Sandberg, S. P., Law, D. C., Weickmann, M., and Hardesty, R. M.: Doppler lidar estimation of mixing height using turbulence, shear and aerosol profiles, *J. Atmos. Ocean. Tech.*, 26, 673–688, doi:10.1175/2008JTECHA1157.1, 2009. 6846, 6864

von Kármán, T.: Progress in the statistical theory of turbulence, *P. Natl. Acad. Sci. USA*, 34, 530–539, 1948. 6837, 6839, 6845

Wagner, R., Mikkelsen, T., and Courtney, M.: Investigation of turbulence measurements with a continuous wave, conically scanning LiDAR, *Tech. Rep. Risø-R-1682(EN)*, Risø DTU, 2009. 6847, 6864

Wagner, R., Courtney, M., Gottschall, J., and Lindelöw-Marsden, P.: Accounting for the speed shear in wind turbine power performance measurement, *Wind Energy*, 14, 993–1004, doi:10.1002/we.509, 2011. 6817

Lidar turbulence measurements review

A. Sathe and J. Mann

Title Page

Abstract

Introduction

Conclusions

References

Tables

Figures

◀

▶

◀

▶

Back

Close

Full Screen / Esc

Printer-friendly Version

Interactive Discussion



Wilczak, J. M., Gossard, E. E., Neff, W. D., and Eberhard, W. L.: Ground-based remote sensing of the atmospheric boundary layer: 25 years of progress, *Bound.-Lay. Meteorol.*, 78, 321–349, doi:10.1007/BF00120940, 1996. 6842

5 Wilson, D. A.: Doppler Radar Studies of Boundary Layer Wind Profiles and Turbulence in Snow Conditions, in: *Proc. 14th Conference on Radar Meteorology, Tucson, USA, 191–196, 1970.* 6825, 6827, 6828, 6851, 6866

Wyngaard, J. C.: *Turbulence in the Atmosphere*, Cambridge University Press, NY, 2010. 6833, 6843, 6848

10 Wyngaard, J. C. and Coté, O. R.: The budgets of turbulence kinetic energy and temperature variance in the atmospheric surface layer, *J. Atmos. Sci.*, 28, 190–201, doi:10.1175/1520-0469(1971)028<0190:TBOTKE>2.0.CO;2, 1971. 6832

Xia, H., Sun, D., Yang, Y., Shen, F., Dong, J., and Koboyashi, T.: Fabry-perot interferometer based mie doppler lidar for low tropospheric wind observation, *Appl. Optics*, 46, 7120–7131, doi:10.1364/AO.46.007120, 2007. 6853

Table 1. Grouping of the past studies according to the estimated turbulence quantity using a lidar.

No.	Quantities Estimated	List of references	Total
1	Turbulent kinetic energy dissipation rate, ε	Kunkel et al. (1980); Gal-Chen et al. (1992); Frehlich et al. (1994); Banakh et al. (1995b, 1996); Frehlich (1997); Banakh et al. (1997); Banakh and Smalikho (1997a,b); Frehlich et al. (1998); Banakh et al. (1999); Drobinski et al. (2000); Frehlich and Cornman (2002); Davies et al. (2004, 2005); Collier et al. (2005); Banakh and Werner (2005); Smalikho et al. (2005); Frehlich et al. (2006); Frehlich and Kelley (2008); Davis et al. (2008); Frehlich et al. (2008); Lothon et al. (2009); Banakh et al. (2010); O'Connor et al. (2010); Chan (2011); Dors et al. (2011); Kristensen et al. (2011, 2012)	29
2	Components of the auto-covariance matrix, R_{ij}	Kunkel et al. (1980); Eberhard et al. (1989); Gal-Chen et al. (1992); Frehlich et al. (1998); Cohn et al. (1998); Davies et al. (2003); Drobinski et al. (2004); Davies et al. (2005); Collier et al. (2005); Banta et al. (2006); Davis et al. (2008); Pichugina et al. (2008); Wagner et al. (2009); Tucker et al. (2009); Mann et al. (2010); Sathe et al. (2011b); Lang and McKeogh (2011)	17
3	Integral turbulent length scale ℓ_{ij} , outer scale of turbulence \mathcal{L}	Frehlich (1997); Frehlich et al. (1998); Cohn et al. (1998); Banakh et al. (1999); Drobinski et al. (2000); Frehlich and Cornman (2002); Davies et al. (2004, 2005); Collier et al. (2005); Banakh and Werner (2005); Smalikho et al. (2005); Lothon et al. (2006); Frehlich et al. (2006); Frehlich and Kelley (2008); Frehlich et al. (2008); Lothon et al. (2009)	16
4	Radial velocity variance, $\langle v_r^2 \rangle$	Eberhard et al. (1989); Gal-Chen et al. (1992); Frehlich (1997); Mayor et al. (1997); Frehlich et al. (1998); Drobinski et al. (2000); Davies et al. (2004); Banakh and Werner (2005); Frehlich et al. (2006); Frehlich and Kelley (2008); Frehlich et al. (2008); Branlard et al. (2013)	12

Lidar turbulence measurements review

A. Sathe and J. Mann

Title Page

Abstract

Introduction

Conclusions

References

Tables

Figures

◀

▶

◀

▶

Back

Close

Full Screen / Esc

Printer-friendly Version

Interactive Discussion



Lidar turbulence measurements review

A. Sathe and J. Mann

Title Page

Abstract

Introduction

Conclusions

References

Tables

Figures

◀

▶

◀

▶

Back

Close

Full Screen / Esc

Printer-friendly Version

Interactive Discussion



Table 1. Continued.

No.	Quantities Estimated	List of references	Total
5	Filtered radial velocity spectrum, $\tilde{F}(k_1)$	Banakh et al. (1997); Mayor et al. (1997); Frehlich et al. (1998); Drobinski et al. (1998); Banakh et al. (1999); Drobinski et al. (2000); Davies et al. (2004); Mann et al. (2009); Sjöholm et al. (2009); Kristensen et al. (2011); Dors et al. (2011); Angelou et al. (2012)	12
6	Filtered radial velocity structure function, $\tilde{D}(r)$ (or $\tilde{D}(r_1)$)	Frehlich et al. (1994); Frehlich (1997); Banakh and Smalikho (1997b); Frehlich et al. (1998); Banakh et al. (1999); Frehlich and Cornman (2002); Davies et al. (2004); Frehlich et al. (2008); Banakh et al. (2010); Chan (2011); Kristensen et al. (2011, 2012)	12
7	One-dimensional spectrum of the components of the wind field, $F_{ij}(k_1)$	Lawrence et al. (1972); Hardesty et al. (1982); Drobinski et al. (2004); Davies et al. (2005); Lothon et al. (2009); O'Connor et al. (2010); Canadillas et al. (2010); Sathe and Mann (2012)	8
8	Third order moments $\langle w^3 \rangle$	Gal-Chen et al. (1992); Cohn et al. (1998); Lenschow et al. (2000)	3
9	Kinematic heat flux, $\langle w'\theta' \rangle$	Gal-Chen et al. (1992); Davis et al. (2008)	2
10	Coherence of the components of the wind field, $\text{coh}_{ij}(k_1)$	Lothon et al. (2006); Kristensen et al. (2010)	2

Lidar turbulence measurements review

A. Sathe and J. Mann

Table A1. Nomenclature.

$C \approx 1.5$	universal Kolmogorov constant
$C_1 \approx 0.5$	Kolmogorov constant related to $F_{11}(k_1)$
$D_{ij}(\mathbf{r})$	velocity structure function
$F_{ij}(k_1)$	one-dimensional velocity spectrum
I	longitudinal turbulence intensity
I_n	Wilson (1970) integrals ($n = 1, \dots, 4$) to estimate the covariances
L_p	range gate length ($c\tau/2$)
$R_{ij}(\mathbf{r})$	cross covariance function
$\mathbf{R} = \mathbf{R}(0)$	covariance matrix
\mathbf{k}	wave vector in the Fourier domain
\mathbf{n}	unit directional vector
\mathbf{r}	separation vector in three dimensions
\mathbf{x}	position vector in three dimensions
$\text{coh}_{ij}(k_1)$	coherence function
$\langle S(v_r) \rangle$	mean Doppler spectra
$\langle u \rangle$	mean wind speed
$\langle w'\theta' \rangle$	sensible heat flux
$\langle u'^2 \rangle$	variance of the u component
$\langle u'v' \rangle$	covariance between the u and v components
$\langle u'w' \rangle$	covariance between the u and w components
$\langle v_r'^2 \rangle$	radial velocity variance
$\langle v'^2 \rangle$	variance of the v component
$\langle v'w' \rangle$	covariance between the v and w components
$\langle w'^2 \rangle$	variance of the w component
$\langle w'^3 \rangle$	third moment of the vertical velocity
\mathbf{v}	wind field vector
$\tilde{D}(\delta)$	filtered radial velocity structure function for a separation distance $d_r\delta$
$\tilde{D}(r)$	filtered radial velocity structure function for a separation distance r
$\tilde{D}(r_1)$	filtered radial velocity structure function for a separation distance r_1
$\tilde{F}(k_1)$	filtered radial velocity spectrum
$\tilde{R}(r)$	filtered covariance function of the radial velocity for a separation distance r
a_n, b_n, a_{mn}, b_{mn}	Fourier coefficients

Title Page

Abstract Introduction

Conclusions References

Tables Figures

◀ ▶

◀ ▶

Back Close

Full Screen / Esc

Printer-friendly Version

Interactive Discussion



Table A1. Continued.

c	speed of light
d_f	focus distance for a c-w lidar and center of the range gate for a pulsed lidar
i, j	indices that take values 1,..,3 and denote the component of the wind field
k_1, k_2, k_3	components of the wave vector along the x_1, x_2, x_3 axes respectively
l	Rayleigh length
r	separation distance along the lidar beam
r_1, r_2, r_3	separation distances along the x_1, x_2, x_3 axes respectively
r_b	lidar beam radius
u	longitudinal component of the wind field in the x_1 direction
v	transversal component of the wind field in the x_2 direction
v_r	radial velocity
w	vertical component of the wind field in the x_3 direction
w_p	pulse width
x_1, x_2, x_3	axes defining the right handed cartesian coordinate system
z	height above the ground
\mathcal{L}	outer length scale of turbulence
$\Phi_{ij}(\mathbf{k})$	three-dimensional spectral velocity tensor
Θ	angle between the lidar beam and the mean wind
α	elevation angle
$\chi_{ij}(k_1, r_2, r_3)$	cross spectra at separation distances r_2 and r_3
δ	angle subtended by two lidar beams in a VAD scanning mode
ℓ_{ij}	integral length scale
$\langle \sigma_s^2 \rangle$	second central moment of the Doppler spectrum (Doppler spectrum width)
$\partial/\partial z$	vertical gradient
ϕ	half-opening angle
ρ	surface air density
τ	pulse duration
θ	azimuth angle
θ_T	surface potential temperature
ε	energy dissipation rate
FWHM	full width half maximum
PPI	plan position indicator
RHI	range height indicator
VAD	velocity azimuth display
c-w	continuous-wave

**Lidar turbulence
measurements
review**

A. Sathe and J. Mann

Title Page

Abstract Introduction

Conclusions References

Tables Figures

◀ ▶

◀ ▶

Back Close

Full Screen / Esc

Printer-friendly Version

Interactive Discussion



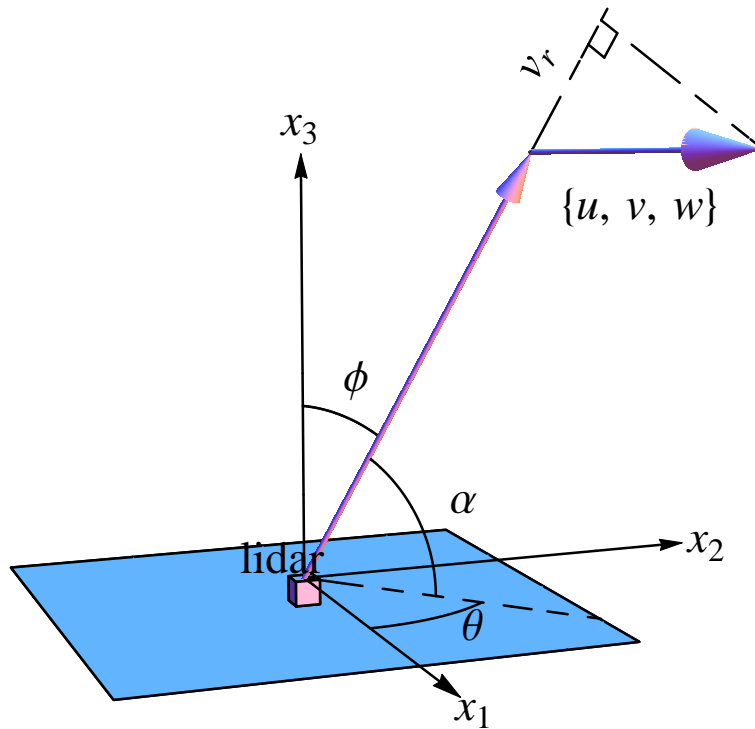


Fig. 1. Schematic of the lidar operating in a staring mode.

Lidar turbulence measurements review

A. Sathe and J. Mann

Title Page	
Abstract	Introduction
Conclusions	References
Tables	Figures
◀	▶
◀	▶
Back	Close
Full Screen / Esc	
Printer-friendly Version	
Interactive Discussion	



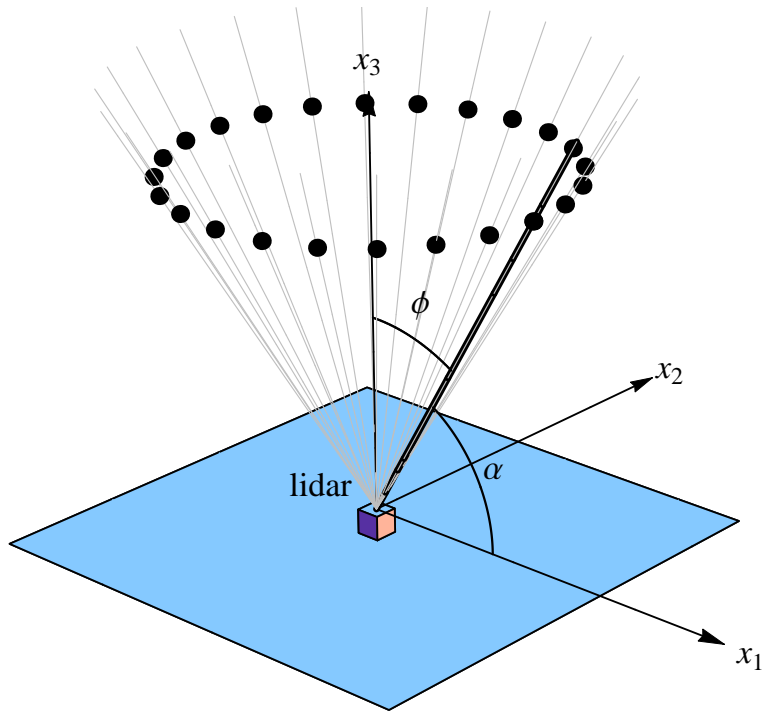


Fig. 2. Schematic of the lidar operating in a VAD scanning mode.

**Lidar turbulence
measurements
review**

A. Sathe and J. Mann

Title Page

Abstract

Introduction

Conclusions

References

Tables

Figures



Back

Close

Full Screen / Esc

Printer-friendly Version

Interactive Discussion



Lidar turbulence measurements review

A. Sathe and J. Mann

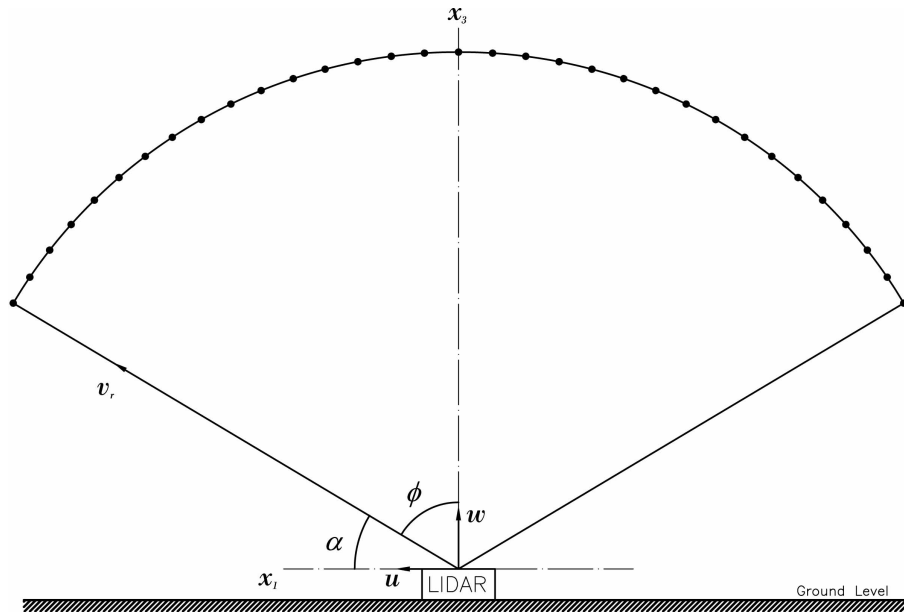


Fig. 3. Schematic of the lidar operating in a RHI scanning mode.

Title Page

Abstract

Introduction

Conclusions

References

Tables

Figures

◀

▶

◀

▶

Back

Close

Full Screen / Esc

Printer-friendly Version

Interactive Discussion



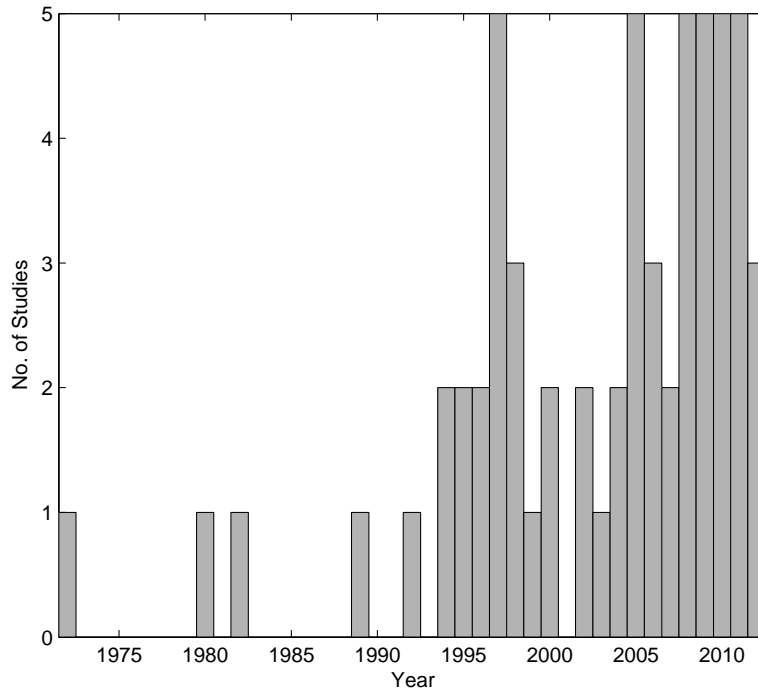


Fig. 4. Number of studies per year on lidar turbulence measurements.

Lidar turbulence measurements review

A. Sathe and J. Mann

Title Page

Abstract

Introduction

Conclusions

References

Tables

Figures

◀

▶

◀

▶

Back

Close

Full Screen / Esc

Printer-friendly Version

Interactive Discussion

